

Electronic Thesis and Dissertation Repository

---

4-26-2022 3:30 PM

## Early Biological Response of Articular Cartilage to Hemiarthroplasty Wear

Debora Rossetti, *The University of Western Ontario*

Supervisor: Johnson, James A., *St. Josephs Hospital - Hand and Upper Limb Center*

A thesis submitted in partial fulfillment of the requirements for the Master of Engineering  
Science degree in Biomedical Engineering

© Debora Rossetti 2022

Follow this and additional works at: <https://ir.lib.uwo.ca/etd>



Part of the [Biomedical Devices and Instrumentation Commons](#)

---

### Recommended Citation

Rossetti, Debora, "Early Biological Response of Articular Cartilage to Hemiarthroplasty Wear" (2022).  
*Electronic Thesis and Dissertation Repository*. 8500.  
<https://ir.lib.uwo.ca/etd/8500>

This Dissertation/Thesis is brought to you for free and open access by Scholarship@Western. It has been accepted for inclusion in Electronic Thesis and Dissertation Repository by an authorized administrator of Scholarship@Western. For more information, please contact [wlsadmin@uwo.ca](mailto:wlsadmin@uwo.ca).

## Abstract

Hemiarthroplasties typically result in accelerated wear of the preserved side of the joint, resulting in suboptimal clinical outcomes and limited longevity. This *in vitro* study investigated the effects of hemiarthroplasty implant curvature on the early biological response of articular cartilage measured by proteoglycan release, histology, and surface morphology. Cartilage from boar radiocarpal joints were worn by metal pins of varying radii of curvature (RoC) using a pin-on-plate wear simulator. Histology and proteoglycan assays showed no significant differences between RoC treatment groups, and proteoglycan assays showed increased proteoglycan release 72 hours after wear testing in worn cartilage specimens compared to control specimens. Field emission scanning electron microscopy showed increased surface damage as RoC decreased. Results suggest that early wear mechanisms smoothen cartilage surface before causing damage. Delayed biological response implied that implant curvature affects early wear mechanics before cartilage biologics. Overall, this study improves our understanding of cartilage wear and cellular response.

### **Keywords**

Hemiarthroplasty, cartilage wear, proteoglycan, histology, surface morphology, field emission scanning electron microscopy, FESEM, curvature, biological response, assay.

## Summary for Lay Audience

Joints that connect and provide movement to our skeletal structure deteriorate with age, use, injuries, and certain diseases; and in some cases, replacement of these joints with implants is required. According to the Canadian Joint Replacement Registry, demand for hip and knee replacements continues to increase in Canada, with about 130,000 surgeries costing \$1.2 billion annually. However, with breaks or fractures it is sometimes not necessary to replace both sides of the joint; for example, in radial head fractures, the most common fracture around the elbow with an incidence rate of 2.5-2.8 for every 10,000 people per year. Hemiarthroplasty replaces only one articulating surface in a joint with an implant, as an alternative to replacing both surfaces in a total arthroplasty. This approach preserves the native joint, reduces costs, and minimises procedure risks and recovery time. However, hemiarthroplasty often results in accelerated cartilage wear of the original side of the joint due to the stiffness of implants relative to cartilage. Studies have suggested that more conforming implant designs reduce contact stress and cartilage wear, even though the biological response of cartilage to implant curvature is still unknown. There is an urgent clinical need for improved hemiarthroplasty implant design.

Our specific research questions are: “How do cartilage cells respond to mechanical wear, and how is this influenced by the implant design?”

The studies used a wear simulator to investigate effects of hemiarthroplasty implant curvature on the biological response of cartilage via proteoglycan release, histology, and field emission scanning electron microscopy. These outcomes assessed the cartilage response to mechanical wear using implant designs of different curvatures. Results showed a delayed biological response of 72 hours, which adds to the literature from a biological perspective, highlighting that cartilage cells respond to mechanical wear with a substantial delay. From that we can deduce that mechanical wear occurs before biological response. Additionally, results showed that implant pin curvature did not affect the biological response as expected. There were also implications that early wear mechanisms first act to smoothen the cartilage before causing damage. Overall, these studies provide a better understanding of early cartilage wear mechanisms.

# Co-Authorship Statement

## **Chapter One**

Literature Review- Debora Rossetti

Writing- Debora Rossetti

Revisions- Debora Rossetti, Frank Beier, Graham King, Jim Johnson

## **Chapter Two**

Study Design- Debora Rossetti, Frank Beier, Dan Langohr, Graham King, Jim Johnson

Testing- Debora Rossetti

Writing- Debora Rossetti

Revisions- Debora Rossetti, Frank Beier, Graham King, Jim Johnson

## **Chapter Three**

Data Analysis- Debora Rossetti, Frank Beier

Statistical Analysis- Debora Rossetti

Writing- Debora Rossetti

Revisions- Debora Rossetti, Frank Beier, Graham King, Jim Johnson

## **Chapter Four**

Writing- Debora Rossetti

Revisions- Debora Rossetti, Frank Beier, Graham King, Jim Johnson

## **Appendix A – sole authorship**

## **Appendix B**

Study Design- Debora Rossetti, Frank Beier, Dan Langohr, Graham King, Jim Johnson

Data Analysis- Debora Rossetti, Frank Beier

Statistical Analysis- Debora Rossetti

## Acknowledgments

Thank you to my supervisor Dr. Jim Johnson for giving me continuous guidance, support, and encouragement. I could not have done it without your positivity and determination. I would also like to thank Dr. Frank Beier, whose expertise was fundamental in formulating the research questions and methodology. Thank you to Dr. Graham King for taking the time to give me feedback and support, I am grateful for your input. And to Dr. Dan Langohr and Dr. John Medley who were always there to give me valuable insights and answer my questions, thank you.

Additionally, I would like to show my appreciation to Caroline O'Neill at Robarts Research Institute for her histology expertise and efficiency; and to Tim Goldhawk and Todd Simpson at Western Nanofabrication Facility for their help in imaging the surface morphology of my samples via FESEM.

I thank you kindly Shannon Seney for your technical help and patience in the lab, you were always there to help when things went sideways. Alana Khayat and Sarah Dedecker, thank you for your inspiring me to continue on from your findings in implant geometry with the hope of improving hemiarthroplasty implants. And to the entire HULC lab, it was a pleasure being part of the team and getting to know you all, thank you for making every day in the lab a positive one.

Last but not least, my parents who have supported me from day one and given me a world of opportunity, I owe everything to you.

# Table of Contents

Abstract.....	ii
Summary for Lay Audience.....	iii
Co-Authorship Statement.....	iv
Acknowledgments.....	v
Table of Contents.....	vi
List of Tables.....	ix
List of Figures.....	x
List of Commonly Used Abbreviations.....	xii
Chapter 1.....	1
1 Introduction to Hemiarthroplasty: Indications and Complications.....	1
1.1 The Function of Articular Cartilage.....	1
1.1.1 Structure and Composition of Articular Cartilage.....	1
1.1.2 Mechanical Function of Articular Cartilage under Load.....	3
1.1.3 Osteoarthritis.....	5
1.1.4 Lubrication of the Synovial Joint.....	5
1.2 Shoulder and Elbow Anatomy, Function and Mechanics.....	6
1.3 Hemiarthroplasty (of the Upper Limb).....	8
1.4 Cartilage Wear.....	10
1.4.1 Quantification of Cartilage Wear.....	10
1.4.1.1 Mechanical Assays.....	11
1.4.1.2 Biological Assays.....	12
1.4.1.3 Surface Morphology.....	13
1.5 <i>In Vitro</i> Studies on the Wear of Cartilage.....	14
1.6 Rationale.....	15

1.7 Objectives and Hypotheses .....	16
1.7.1 Objectives .....	16
1.7.2 Hypotheses .....	16
1.8 Thesis Overview .....	16
Chapter 2.....	17
2 Materials and Methods.....	17
2.1 Materials .....	17
2.2 Methods.....	18
2.2.1 Tissue Preparation.....	18
2.2.2 Wear Testing.....	19
2.2.3 Post-wear Analyses.....	22
2.2.4 Assays .....	24
2.2.4.1 Proteoglycan Assay .....	24
2.2.4.2 Histology .....	26
2.2.4.3 Surface Morphology.....	26
2.2.4.4 Summary.....	27
Chapter 3.....	28
3 Results .....	28
3.1 General Observations.....	28
3.2 Proteoglycan Assay.....	29
3.3 Histology.....	32
3.4 Surface Morphology .....	35
3.5 Summary .....	37
Chapter 4.....	38
4 Discussion .....	38

4.1 Principal Findings .....	38
4.2 Limitations .....	45
4.3 Future Directions .....	47
4.4 Conclusions.....	48
References.....	49
Appendices.....	67
Appendix A – Glossary .....	67
Appendix B – Pilot Studies for Time Point and Concentration Optimization.....	70
Curriculum Vitae .....	72



## List of Tables

Table B-1: <i>The treatments applied to each sample in the pilot studies.</i> .....	70
---	----

## List of Figures

Figure 1-1: <i>Articular cartilage layers.</i> .....	3
Figure 1-2: <i>Pressures in the synovial joint.</i> .....	4
Figure 1-3: <i>Elbow and forearm anatomy.</i> .....	7
Figure 1-4: <i>Shoulder anatomy, and the glenohumeral joint.</i> .....	8
Figure 1-5: <i>Radial head replacement.</i> .....	9
Figure 2-1: <i>Stainless steel pin implant models of varying radii of curvature.</i> .....	18
Figure 2-2: <i>Cartilage plug drilled using a 25mm diamond-tip hole drill-bit.</i> .....	19
Figure 2-3: <i>The specifics of the testing set up of the pin-on-plate wear simulator against cartilage specimens.</i> .....	21
Figure 2-4: <i>Wear testing set up.</i> .....	22
Figure 2-5: <i>A summary of treatment allocations for the worn cartilage specimens.</i> .....	23
Figure 2-6: <i>Calibration curve for calculating proteoglycan concentrations.</i> .....	25
Figure 3-1: <i>A typical wear track on a worn cartilage specimen.</i> .....	29
Figure 3-2: <i>Plot of average proteoglycan concentration 24 hours after wear testing for each implant radius of curvature (RoC) treatment group.</i> .....	30
Figure 3-3: <i>Plot of average proteoglycan concentration 72 hours after wear testing for each implant radius of curvature (RoC) treatment group.</i> .....	31
Figure 3-4: <i>Histology images (n=3) of cartilage specimens 24 hours after wear with different pin geometry's and stained with Safranin-O/Fast Green.</i> .....	33
Figure 3-5: <i>Histology images (n=3) of cartilage Specimens 72 hours after wear with different pin geometry's and stained with Safranin-O/Fast Green.</i> .....	34

Figure 3-6: <i>Field emission scanning electron microscopy images of cartilage surfaces worn with different pin geometries.</i> .....	36
Figure 4-1: <i>Photograph from Verberne et al. capturing the boundary of a wear track on the cartilage surface<sup>22</sup>.</i> .....	43
Figure 4-2: <i>FESEM images of cartilage surfaces worn with (b-d) 5.10-9.35mm pins and the unworn (f) control.</i> .....	44
Figure B-1: <i>Plot of pilot studies assessing proteoglycan concentrations at 0, 12, and 24 hours after wear testing, different concentrations/dilutions, and pin geometries.</i> .....	71

## List of Commonly Used Abbreviations

ADAMTS	A disintegrin and metalloproteinase with thrombospondin motifs
ANOVA	Analysis of Variance
DMEM	Dulbecco's Modified Eagle Medium
FESEM	Field Emission Scanning Electron Microscopy
GAG	Glycosaminoglycan
MMP	Matrix metalloproteinases
OA	Osteoarthritis
RoC	Radius of curvature
SEM	Scanning Electron Microscopy
sGAG	Sulphated-glycosaminoglycan

## Chapter 1

### 1 Introduction to Hemiarthroplasty: Indications and Complications

*Overview: This thesis has a focus on cartilage wear due to hemiarthroplasty implants articulating against cartilage. This chapter provides an overview of literature concentrating on cartilage wear of hemiarthroplasties, and techniques for measuring said cartilage wear. It introduces the function and mechanics of articular cartilage. Furthermore, the application of this work to elbow and shoulder hemiarthroplasties is reviewed, although the current studies have relevance to hemiarthroplasties of all joints. Objectives, hypotheses, and a thesis overview are included in the final pages of Chapter 1.*

#### 1.1 The Function of Articular Cartilage

Articular cartilage is a porous, soft connective tissue. It covers the articulating bone end surfaces in synovial joints. It is viscoelastic as it exhibits viscous and elastic properties when undergoing deformation. Also known as hyaline cartilage, it functions to allow for the motion of articulating surfaces by providing a smooth lubricated surface and aiding load transmission while generating minimal friction<sup>1</sup>. Cartilage provides joints with the ability to resist wear, bear loads, and absorb shocks under repeated loading, friction, and trauma<sup>2,3</sup>.

##### 1.1.1 Structure and Composition of Articular Cartilage

Articular cartilage is constantly being subjected to harsh mechanical conditions. It has no direct blood supply and receives nutrients from the synovial fluid and subchondral bone, and this explains its limited repair and growth mechanisms<sup>1,4</sup>. The complexity of cartilage structure makes medical repair and treatments difficult. Because of this, maintaining healthy articular cartilage is essential to a healthy, functioning joint.

Chondrocytes are specialised cells that secrete cartilage matrix and become embedded in it. They are the main cell type that makes up articular cartilage, regulating the dense extracellular matrix (ECM) turnover and maintaining tissue homeostasis<sup>5</sup>. The ECM consists primarily of water, collagen, proteoglycans, other non-collagenous proteins, and glycoproteins<sup>1,6</sup>.

Cartilage has a biphasic nature, meaning it consists of both solid and fluid phases<sup>1</sup>. The fluid phase is composed mainly of water, making up to 80% of the wet weight of articular cartilage. Water in the ECM faces a strong frictional resistance to flow, resulting in the low permeability of cartilage. This frictional resistance combined with water pressurisation in the matrix is a major contributor to its load-bearing properties. The solid phase is composed of collagen fibrils and proteoglycans<sup>2,7</sup> – the two main load-bearing macromolecules in cartilage. Proteoglycans have a protein core bound to multiple glycosaminoglycans and oligosaccharides<sup>8,9</sup>, an example being aggrecan, which controls the osmotic properties of articular cartilage through negative electrostatic repulsion forces and in turn, its resistance to compressive loads<sup>1</sup>. Collagen is the most prevalent structural protein found in animal connective tissues - type II collagen is the most common type of collagen (90-95%) found in the ECM of articular cartilage<sup>1</sup>. These are the major components that give articular cartilage its properties to serve its function.

Four zones make up articular cartilage, each differing in structure, distribution, and relative composition, as shown in Figure 1-1:

- The superficial zone has thin, tightly packed collagen fibers arranged into layers parallel to the articular surface and chondrocytes appear flattened. This makes up 10-20% of articular cartilage volume and functions to protect deeper cartilage layers from shear stresses<sup>1</sup>.
- The transitional zone has less distinct orientation, thicker collagen fibrils, rounded chondrocytes, and proteoglycans are aligned obliquely. This makes up 40-60% of articular cartilage volume and functions to provide resistance to compressive forces<sup>1</sup>.

- The deep zone has collagen fibrils perpendicular to the articular surface, and round chondrocytes arranged in columns. This makes up 30% of articular cartilage and has the most contribution to compressive force resistance. This zone has a higher concentration of proteoglycans, and lower concentration of water compared to the other zones<sup>1</sup>.
- The calcified zone has collagen fibers that are radially oriented in tightly packed bundles. This zone anchors the cartilage to the subchondral bone.

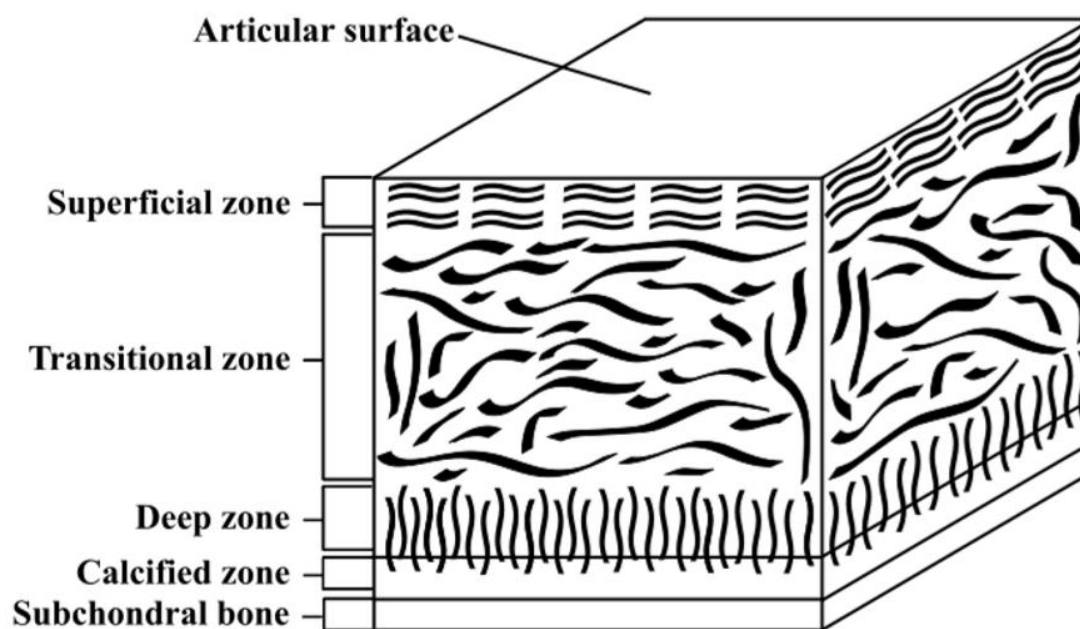


**Figure 1-1:** Articular cartilage layers.

*The cross-section of collagen fiber architecture in articular cartilage, showing the four zones that cartilage is divided into based on organisation and function. (Used with permission of Alana Khayat<sup>10</sup>).*

### 1.1.2 Mechanical Function of Articular Cartilage under Load

Considering mechanical properties is crucial when studying the function of cartilage. In biomechanical terms, the functional characteristics of articular cartilage are largely

dependent on its multiphasic nature<sup>9-13</sup>. Because of this nature, cartilage reduces articular stresses not only in itself but in the subchondral bone, as well<sup>2,14,15</sup>.

Figure 1-2 shows how cartilage helps synovial joints uphold minimal contact pressures. Biphasic contact between opposing cartilage surfaces of a joint maximises articular contact area, resulting in decreased stress concentrations and contact pressures<sup>16</sup>.

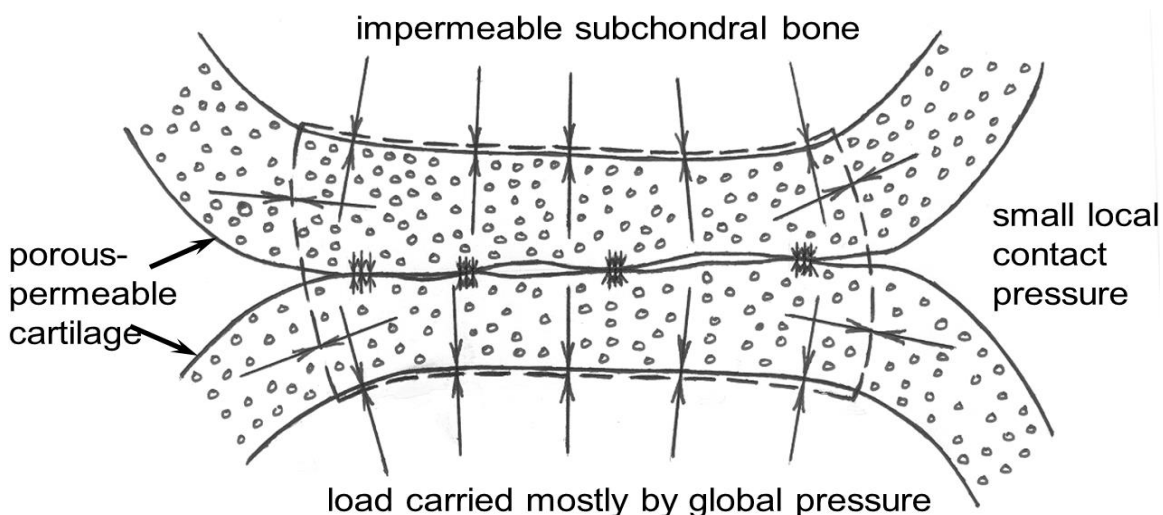


**Figure 1-2:** *Pressures in the synovial joint.*

*The small arrows at the articulation of cartilage represent small, local contact areas. The large arrows between cartilage and subchondral bone show load carried mostly by global pressure. (ME 598 Engineering Biomechanics lecture notes, reproduced with permission of Professor JB Medley, Department of Mechanical and Mechatronics Engineering, University of Waterloo).*

An important characteristic of cartilage is its permeability, which is its resistance to fluid flow. When subject to compressive loads, the fluid phase dissipates most of the load force, the permeability decreases and thus, flow out of the cartilage also decreases<sup>7</sup>. Unconfined and confined compression testing is often used to determine and evaluate biomechanical properties of articular cartilage, including the permeability, Young's modulus ( $E$ ) and aggregate modulus ( $HA$ )<sup>11</sup>. The aggregate modulus is a measure of the stiffness of the tissue at equilibrium when all fluid flow is halted. Compression tests have shown human cartilage to have an aggregate modulus range from 0.50 to 0.90 MPa and a Young's



modulus range from 0.45 to 0.90 MPa<sup>12,13</sup>. One indentation study showed a higher Young's modulus of 1.79 MPa in instantaneous response for bovine cartilage<sup>14</sup>.

Indentation testing of cartilage determined an equilibrium and instantaneous Poisson's ratio to be 0.46 and 0.50, respectively. Poisson's ratio of cartilage is typically below 0.4 and often approaches zero<sup>2,15</sup>. As for the coefficient of friction, static and dynamic loading has revealed values of 0.2-0.4 for static loading over several hours, and 0.002-0.200 for dynamic loading<sup>16</sup>.

Acute, traumatic injury to the cartilage may heal itself depending on the nature and depth of the damage. However, mechanical impact to the cartilage may also lead to loose fragments of cartilage and bone in the synovial joint. This can hinder joint motion, as well as cause more damage to the cartilage surface by increased third body wear. All in all, fatigue is the inevitable cause of progressive cartilage degeneration, yet the rate of degeneration greatly depends on numerous factors, such as, age and activity level<sup>9</sup>.

### 1.1.3 Osteoarthritis

Osteoarthritis (OA) is a degenerative joint disease that affects millions worldwide. In severe cases, OA causes formation of osteophytes, inflammation, degeneration of ligaments and menisci, and ultimately, stiffness, pain, mechanical locking of joints, and disability<sup>17</sup>. It has multifactorial etiology, and wear and degradation of cartilage are known contributors<sup>18</sup>. As the cartilage degrades, the Young's modulus decreases and permeability increases. This shift reduces the ability of cartilage to serve its function.

### 1.1.4 Lubrication of the Synovial Joint

For movement of the synovial joint, proper lubrication is required to provide low frictional properties of a coefficient of friction on the order of ~0.01 or less<sup>19,20</sup>. Improper lubrication of the joints results in a greater coefficient of friction and causes increased cartilage wear<sup>19,21-24</sup>. Synovial fluid is an ultrafiltrate of plasma to which synoviocytes (cells within the synovial membrane) add hyaluronan and lubricin<sup>25</sup> and it functions to provide lubrication and nutrition to synovial joints<sup>26</sup>.

Research has shown that lubricin, a 227 kDa glycoprotein, can lubricate non-cartilaginous surfaces as effectively as synovial fluid in the boundary mode<sup>27,28</sup>. Bovine serum is typically the recommended lubricant for *in vitro* wear testing because it closely mimics wear rates and mechanisms seen in the *in vivo* environment<sup>29</sup>.

## 1.2 Shoulder and Elbow Anatomy, Function and Mechanics

*While this thesis is generic in that the overall aim is to examine some fundamental aspects of cartilage wear with hemiarthroplasty implants for all joints involved (as discussed ahead), the application of hemiarthroplasty for shoulder and elbow is highlighted in this chapter. Hence this section describes the shoulder and elbow.*

The upper limb is essential for most activities in life, from daily movements to precise detailed motions to simply giving one the ability to balance. The upper limb provides us with a wide range of motion, and without proper function, any form of activity becomes extremely difficult<sup>30</sup>. It is made up of several joints that connect the shoulder to the humerus to the forearm, the radius and ulna, to the hand. These work together to pass on forces from the shoulder to the wrist, and vice versa. This is crucial for precise hand movement and placement for activities of daily living.

A major stabilising component of the elbow is the ulnohumeral joint (where the trochlea of the humerus articulates with the greater sigmoid notch of the ulna) which has a “tongue and groove” configuration for a tight fit. Additionally, the spherical capitellum articulates on the concave radial head allowing for the wide range of motion of the elbow and forearm<sup>31-33</sup>. The proximal and distal radioulnar joints are responsible for the rotation of the radius about the axis of the ulna - turning the hand from palm up to palm down position. Damage to any of the elbow’s components can decrease mobility and stability. Figure 1-3 displays the elbow joint anatomy, as well as motions.

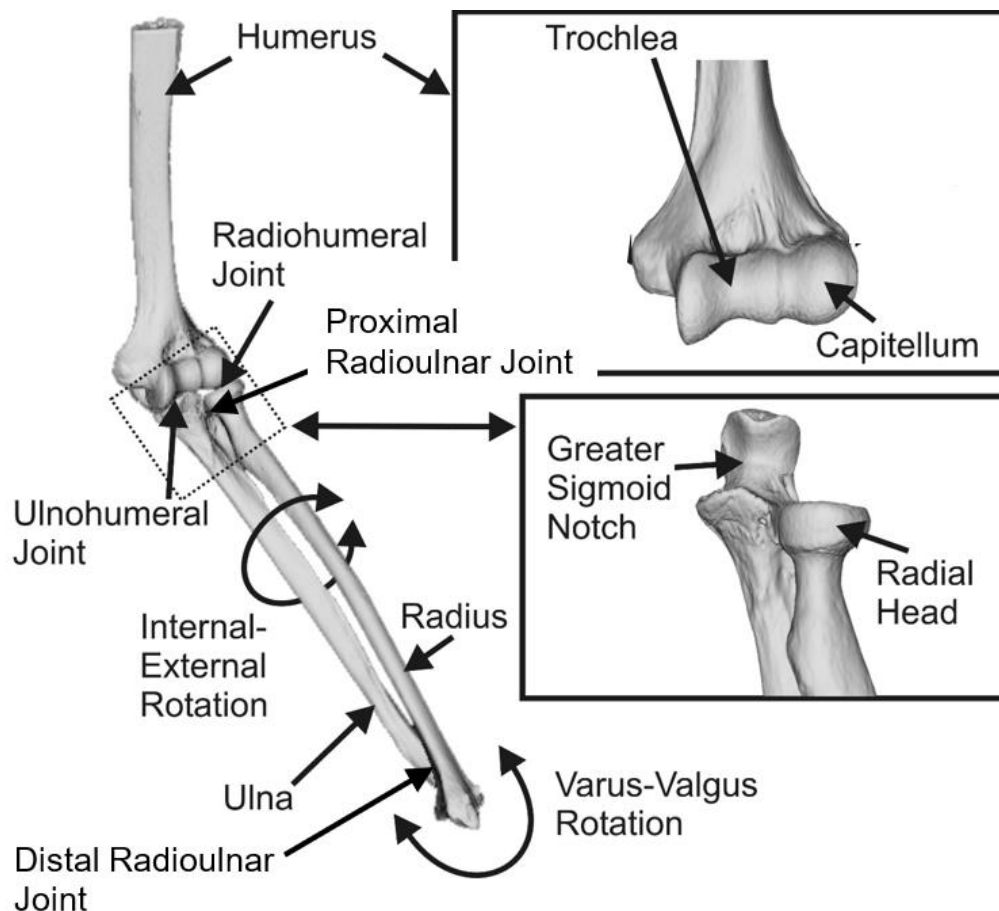


**Figure 1-3:** *Elbow and forearm anatomy.*

*The labelled elbow joints – ulnohumeral, radiohumeral, and the proximal and distal radioulnar joints. The elbow can rotate as varus-valgus rotation or internal-external rotation. (Used with permission of Alana Khayat<sup>10</sup>).*

The shoulder joins the clavicle, scapula and humerus with two joints (Figure 1-4). The shoulder is less stable than the elbow, and thus dislocation is more common. The glenohumeral joint is where the glenoid, a flat surface of the scapula, meets the humeral head. These together form the shoulder ball-in-socket joint. This articulation allows for most shoulder motions. The clavicle, also known as the collar bone, forms a joint with the scapula.

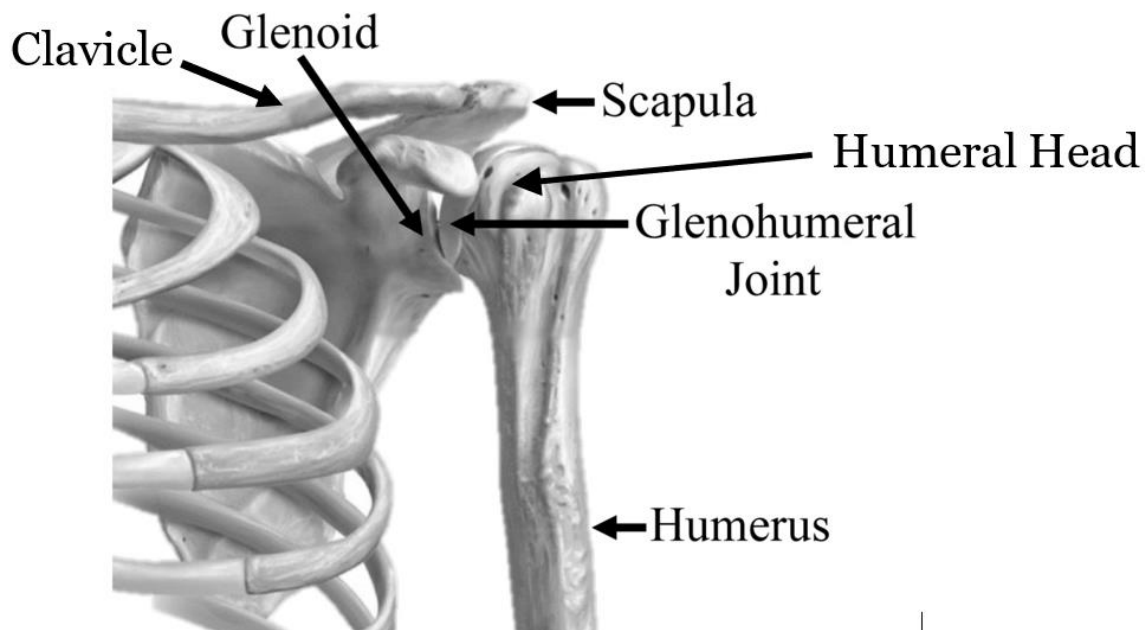


**Figure 1-4:** *Shoulder anatomy, and the glenohumeral joint.*

*The labelled bones in the shoulder joint. (Used with permission of Alana Khayat<sup>10</sup>).*

### 1.3 Hemiarthroplasty (of the Upper Limb)

Complete joint replacement implant systems are typically the prescribed treatment for end stage arthritis and some periarticular fractures. Hemiarthroplasty is an alternative that preserves native tissue, requires less invasive implantation techniques, reduces patient morbidity and minimizes cost<sup>34</sup>. A partial replacement (hemiarthroplasty) only replaces one of the articulating surfaces of a joint. This a viable alternative in cases where only one of the joint surfaces is damaged or irreparable, for example, in the case of a radial head, distal humerus, or proximal humerus fracture (Figure 1-5).

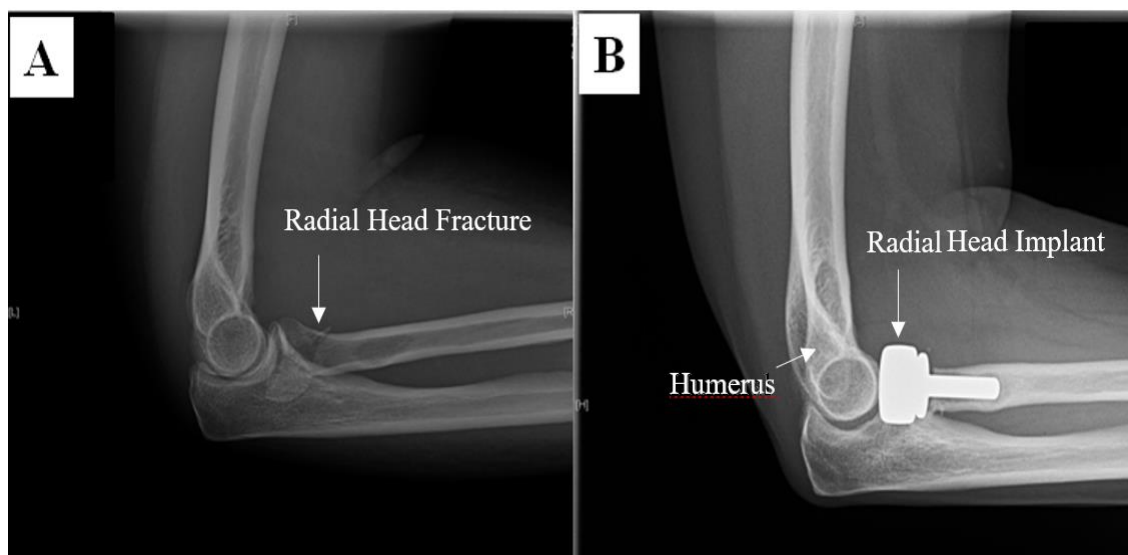


**Figure 1-5:** *Radial head replacement.*

*A routine hemiarthroplasty operation A) A radiograph showing the radial head fracture in the right elbow before the operation; B) A radiograph showing the hemiarthroplasty implant articulating against the capitellum of the humerus post-operation. (Used with permission of Alana Khayat<sup>10</sup>).*

Although still with limited success, hemiarthroplasties of the lower body<sup>35-40</sup> have shown a greater clinical success than those of the upper body<sup>41-45</sup>. This may be due to the comparatively invasive surgical approach for implantation, as well as, to suboptimal implant design<sup>46-48</sup>. One possibility is that hip and knee hemiarthroplasty implant designs represent a more accurate replication of the native anatomy whereas shoulder and elbow hemiarthroplasty implants are yet to show maximal contact area to the articulating cartilage<sup>49</sup>. For instance, hemiarthroplasty as radial head replacement has less clinical success due to inferior contact mechanics at the joint<sup>50-52</sup>. Hemiarthroplasty procedures have suboptimal clinical outcomes and limited longevity due to wear of the articular cartilage. As such, they are generally performed on older, less active patients despite their simplified surgical approach<sup>51,53</sup>.

It has been reported that the high stiffness of metal implants used in hemiarthroplasties increases contact stress, and as a result, cartilage wear<sup>55,56</sup>. One study compared contact area of the native joint to that with a metal unipolar radial head and reported the contact of

the hemiarthroplasty was two thirds that of the native articulation<sup>57</sup>. A decrease in contact area results in an increased contact pressure, which is linked to increased cartilage degeneration<sup>33</sup>. High contact pressures also cause an increased release of degenerative enzymes that act to reduce articular cartilage stiffness and elasticity<sup>58</sup>. Compression trauma and fissuring is known to result in chondrocyte death<sup>59-61</sup>. Additionally, current implant geometries do not replicate the shape of the bone which they replace, altering the congruity with the preserved native articulation. This adds to the cartilage degeneration already caused by high contact pressures<sup>56,62,63</sup>. There is a positive correlation between articular cartilage damage and the amount of time since hemiarthroplasty<sup>50,64,65</sup>.

The demand for upper limb hemiarthroplasties is high due to a frequent occurrence of unreliable fractures such as radial head, distal humerus, and proximal humerus<sup>55,66</sup>. These patients tend to be younger, more active, and have more years to live with the implant. This raises the probability of severe cartilage wear, after which a total arthroplasty is required.

## 1.4 Cartilage Wear

### 1.4.1 Quantification of Cartilage Wear

Wear is the removal of material from a surface resulting from chemical or mechanical action between the contact surfaces<sup>16</sup>. Wear mechanisms consist of surface adhesion, abrasion, fatigue, and corrosion. Quantifying cartilage wear can be a challenge because of the high-water content which influences the geometric and gravimetric measurements of wear. For this reason, studies have deemed surface topography a preferred method over gravimetric wear measurements. Protocols have been framed by multiple studies both *in vivo* and *in vitro*<sup>16,67-73</sup>.

Impressively, weight-bearing joints routinely carry up to ten times body weight under normal loading conditions. Such forces translate to contact stresses of 5-10 MPa<sup>74</sup>. Cartilage has a critical stress threshold of 15-20 MPa after which chondrocyte death and damage to the collagen fiber organisation is observed<sup>74</sup>. High contact stresses are associated with a high coefficient of friction at the articulation of the implant against the opposing cartilage, and greater cartilage wear. Friction shear stress is the product of contact

stress and coefficient of friction. Studies have shown a significant correlation between friction shear stress (FSS) and cartilage wear volume<sup>75,76</sup>.

#### 1.4.1.1 Mechanical Assays

McGann et al. investigated *in vitro* methodologies of quantifying cartilage wear<sup>67</sup>. They compared semi-quantitative visual analysis, quantification by change in surface roughness, and quantification by mass of collagen removed as a function of surface area. It was reported that mass analysis by high performance liquid chromatography (HPLC) analysis of hydroxyproline should remain the ‘gold standard’; however, visual analysis by India ink can be a less expensive, quicker, as well as accurate, alternative. Numerous studies have utilised India ink as a visual method for quantifying wear, as it adheres at different intensities of pigmentation to fibrillated cartilage. This can be identified and quantified by a Matlab computer technology<sup>47,67</sup>. The surface roughness method was deemed less accurate than the other two methods, although changes in surface morphology were still noted.

Chan et al. investigated friction and wear of cartilage articulating against four common orthopaedic biomaterials – alumina ( $\text{Al}_2\text{O}_3$ ), cobalt chromium (CoCr), stainless steel (SS), and crosslinked ultra-high-molecular-weight polyethylene (UHMWPE)<sup>68</sup>. The methodology used was reciprocal sliding of the implants against the cartilage by a pin-on-disc tribometer. Standard mass quantifications assess dry mass of the worn material; however, hydration is highly important in articular cartilage. Instead, cartilage wear was quantified by mass removed from the cartilage into the lubricating bath and normalised to the mean contact pressure and total sliding distance.

Oungouliau et al. measured the wear response of articular cartilage to two cobalt-chromium alloys and stainless steel<sup>23</sup>. Friction measurements were compared between the different materials. Surface roughness was also a variable for the cobalt-chromium alloys.

Khayat and Dedecker both measured early *in vitro* cartilage wear via a 3D non-contact scanner in their studies<sup>10,77</sup>. Wear was quantified by volume of material removed and the average depth of the wear tracks. Specimens were scanned before and after testing and then

the images were aligned in Meshlab. An inter-surface distance algorithm computed the total wear volume. Average wear depth was then calculated as the volumetric wear divided by the contact area.

#### 1.4.1.2 Biological Assays

The aforementioned study by Chan et al. also used protein wear assays and histology, in addition to the mechanical assays, in assessment of cartilage wear by different biomaterials<sup>68</sup>. After wear testing, the phosphate buffer saline (PBS) in which wear tests were performed was centrifuged. The solution was then assayed with a Bicinchoninic acid (BCA) assay and an enzyme-linked immunosorbent assay (ELISA). The BCA quantified total protein in a sample and the ELISA quantified superficial zone protein (SZP), a boundary lubricant found in the cartilage surface also known as lubricin. Immunohistochemistry was used to confirm the distribution of lubricin in the worn cartilage compared to a control. Generally, lubricin is a good indication of early cartilage wear because it is removed from the cartilage surface during wear<sup>24</sup>.

Proteoglycans are glycosylated proteins that make up much of the ECM of cartilage and are synthesized by chondrocytes, secreted into the ECM, and then undergo breakdown/release<sup>1</sup>. They have a protein backbone and glycosaminoglycan (GAG) side chains, and over 95% of GAG is sulphated in articular cartilage<sup>78</sup>. Proteoglycan synthesis is a measure of chondrocyte function in the cartilage as proteoglycan content is one of the main features of cartilage integrity<sup>79</sup>. Aggrecan is an abundant proteoglycan core protein and is the main proteoglycan found in articular cartilage - it plays a large role in cartilage repair. Proteoglycan content or release are common evaluations used in many studies for cartilage wear assessment, particularly early wear<sup>23,78,80,81</sup>. An increase in proteoglycan released into the serum surrounding the cartilage indicates increased cartilage damage. Guilak et al. in 1994 assessed the effects of compressive stress on the rate of proteoglycan synthesis in bovine articular cartilage<sup>81</sup>. They assessed total proteoglycan release with sulphated-GAG (sGAG) assays which uses the dye 1,9-dimethylmethylene blue (DMMB) to colorimetrically quantify total proteoglycan concentration<sup>82</sup>.



Hydroxyproline (HYP) content is commonly used as marker of collagen matrix and to measure the extent of wear during *in vitro* experiments<sup>70,83</sup>. It is a stabilising component of collagen. The majority gets dissolved into lubricant during testing so both the cartilage and lubricant need to be analysed to quantify cartilage wear by hydroxyproline assay.

Matrix metalloproteinase (MMP) 13 is a protease that breaks down collagen and proteoglycans, and thus causes cartilage degradation. It is a strong marker for OA and an encouraging target for treatment of OA<sup>84</sup>. Wang et al. found that inhibiting MMP13 resulted in decelerated cartilage wear in mice<sup>85</sup>. An ELISA assay can be used to quantify MMP13 protein to indicate the progression of cartilage wear.

Proteases ADAMTS-4 and ADAMTS-5 are also involved in proteoglycan degradation in OA and rheumatoid arthritis<sup>86</sup>. They are enzymes that break down aggrecan resulting in a decrease in the cartilage's ability to resist compressive forces<sup>87</sup>. Research has showed that inhibition of ADAMTS-4 and ADAMTS-5 can prevent the aggrecan degradation seen in early-stage OA<sup>88-91</sup>. ELISA assays can quantify ADAMTS-4 and ADAMTS-5 to assess the cartilage degradation occurring due to aggrecan break down.

Histology can be used to examine the surface condition and the structure and organization of cells and tissues of cartilage under a microscope. Scoring methods can be used to quantify the damage of the cartilage – the Mankin method<sup>92</sup> and Osteoarthritis Research Society International (OARSI)<sup>93-95</sup> scoring methods are two of the most common. Safranin-O/Fast Green stains for proteoglycans and is often used to understand the extent of cartilage wear<sup>23,96-99</sup>. The intensity of this stain is proportional to proteoglycan content<sup>96</sup>.

### 1.4.1.3 Surface Morphology

Imaging the surface of articular cartilage can expose the changes in articular cartilage and wear particles following wear testing<sup>100-102</sup>. Directly observing changes in the surface of cartilage is one way to see early wear mechanisms. Visual observations of the cartilage surface can give many indications of how the wear is occurring as well as the extent of the wear. Another way is through analysing wear particles that were removed from the

cartilage surface during wear testing<sup>103</sup>. This typically involves using an algorithm for particle analysis examining size, shape, and surface morphology<sup>100</sup>.

Scanning electron microscopy is the conventional imaging generally used to capture cartilage surface morphology<sup>100</sup>.

## 1.5 *In Vitro* Studies on the Wear of Cartilage

A limited number of studies have examined the wear of cartilage *in vitro*.

Khayat examined the effect of both hemiarthroplasty implant geometry and material on early *in vitro* cartilage wear<sup>10</sup>. Implant pin models of varying radii of curvature were employed against bovine cartilage explants using a pin-on-plate wear simulator. Cartilage wear was quantified using a 3D scanner. It was found that as the radii of curvature increased, and thus the contact area increased, the cartilage wear decreased. However, this trend showed that varying the radii of curvature at lower radii had less of an effect on cartilage wear than when varying the radii of curvature at higher radii. In a related study, the effect of implant material (stiffness) was assessed. Stainless steel, titanium, polyether ether ketone (PEEK), high density polyethylene (HDPE), and ultra-high molecular weight polyethylene (UHMWPE) were tested. The results concluded that stiffness of the material did not affect articular cartilage wear, at least for this range of stiffness.

Dedecker investigated the effect of low stiffness biomaterials on cartilage wear with a finite element study<sup>77</sup>. It was reported that as stiffness decreased, the contact stress levels decreased, as well as volumetric cartilage wear assessed via scanning. A second study on cartilage wear focused on the biomaterials Bionate-Low, Bionate-Mid, Bionate-High, and ceramic<sup>77</sup>. Results indicated that Bionate-High's elevated stiffness generated greater volumetric cartilage wear. Bionate-Low and Bionate-Mid were favourable over Bionate-High.

These studies employed an assessment of mechanical wear solely and hence it is not clear if the wear occurring was due to mechanical and/or biological responses in cartilage.

## 1.6 Rationale

This research investigates the biological responses of articular cartilage to different hemiarthroplasty implant curvatures.

Hemiarthroplasties present a theoretically ideal alternative to total arthroplasties in upper limbs (elbow, shoulder) as they minimize invasiveness of the system, reduce costs, and preserve bone and joint. Additionally, they require a less extensive surgical procedure with reduced risk of complications. However, the issue with hemiarthroplasties is that they typically result in accelerated wear of the preserved cartilage, causing reduced function and quality of life.

There is strong evidence that the conformity of the implant to the native cartilage strongly affects contact patterns in hemiarthroplasty systems<sup>104,105</sup>. However, the influence of implant curvature on the biological response of cartilage is not clear to-date. It is unknown whether relationships are a gradual trend or bounded by thresholds. These factors must be better understood for improved design of hemiarthroplasty implants to optimize their long-term results.

These following studies in this thesis will elucidate the relationship between implant design and biological cartilage wear responses. By performing biological assays and surface analysis, the studies will provide a better understanding of the causation of wear, and whether early wear mechanisms have a mechanical or biological basis, or both. An important question to ask is: “how do the cartilage cells respond to mechanical wear and is this influenced by the geometry of the implant?”

If we can understand the underlying factors that cause this wear of cartilage then hemiarthroplasty implant designs can be improved to reduce this wear, which would in turn save costs to healthcare while producing improved patient outcomes.

## 1.7 Objectives and Hypotheses

### 1.7.1 Objectives

1. To investigate the biological responses of articular cartilage by five different hemiarthroplasty stainless steel implant curvatures via measurement of proteoglycan release, histology, and field emission scanning electron microscopy;
2. To compare the cartilage biological responses at 24 hours and 72 hours after wear testing.

### 1.7.2 Hypotheses

1. Increasing implant curvature, and thus contact area, will decrease biological responses from the articular cartilage;
2. The biological responses of cartilage will be greater at 72 hours after wear testing compared to 24 hours.

## 1.8 Thesis Overview

The following chapters detail *in vitro* studies of the effect of hemiarthroplasty implant curvature on the biological response of articular cartilage. Chapter 2 illustrates the materials and methodologies of the study. Chapter 3 presents the results for each of the mentioned objectives. Lastly, Chapter 4 discusses the results and limitations, explores future research directions, and draws conclusions.

## Chapter 2

### 2 Materials and Methods

*Overview: This chapter focuses on the materials and methods of in vitro studies investigating the effect of a metal hemiarthroplasty implant on the early biological markers of cartilage wear. We also studied the effect of implant curvature on markers of cartilage wear. Stainless steel pins of varying curvature were articulated against cartilage explants in a pin-on-plate wear simulator. Proteoglycan concentrations, histological imaging, and surface morphologies were assessed.*

#### 2.1 Materials

The hemiarthroplasty implant models used were five stainless steel pins of varying radii of curvature (RoC). RoC ranged from a hemispherical curvature (RoC = 4.70 mm) to nearly planar (RoC = 11.70 mm) as shown in Figure 2-1. The pins were convex as they were mimicking a hemiarthroplasty implant that would be used to replace a convex bone surface to articulate against a concave bone surface such as a capitellar or humeral head implant. The pins were custom-made from AISI 304 stainless steel at University Machine Services at the University of Western Ontario (London, ON, Canada). The pins had a Young's modulus of 200 GPa and were polished to 1.9  $\mu\text{m}$  surface roughness  $R_a$  as confirmed by the University Machine Services. All pins were soaked in diluted isopropyl alcohol solution to ensure the surfaces were free from any debris and embedded particles prior to use.

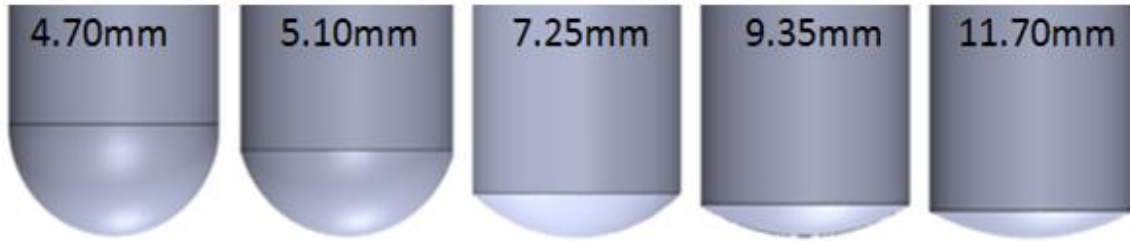


**Figure 2-1:** *Stainless steel pin implant models of varying radii of curvature.*

*Hemiarthroplasty implant models with radii of curvatures shown. Young's Modulus ( $E$ ) = 200 GPa, Surface Roughness ( $R_a$ ) = 1.9  $\mu\text{m}$ . (Used with permission of Alana Khayat<sup>10</sup>).*

## 2.2 Methods

### 2.2.1 Tissue Preparation

12 radiocarpal joints from the forelimbs of freshly slaughtered mature male boars were obtained from a local abattoir (Mount Brydges Abattoir, ON) within 2 hours of death.

Five (5) mm deep cylindrical plugs of fresh articular cartilage and the underlying subchondral bone were extracted from the intermediate carpal bone in the radiocarpal joint using a 25 mm diameter diamond-tip hole drill-bit (Figure 2-2). One specimen was obtained from each of the 12 joints. The boar's radiocarpal joint refers to the joint between the radius and the proximal row of carpal bones. Cartilage harvested had a concave surface.

Between harvesting and the initiation of wear testing, cartilage specimens were submerged in phosphate buffered saline (PBS) to prevent dehydration.

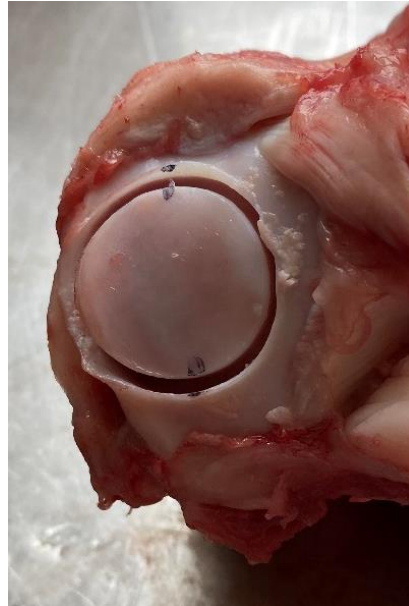


**Figure 2-2:** *Cartilage plug drilled using a 25mm diamond-tip hole drill-bit.*

*An example of a five (5) mm deep cartilage plug drilled using a 25 mm diamond-tip hole drill-bit for preliminary testing purposes.*

Instant Tray Mix (Lang Dental Mfg Co., Inc., Illinois) was used to cement the cartilage plugs into custom jigs. The jigs were then positioned to align the flexion-extension axis of the cartilage with the direction of wear.

### 2.2.2 Wear Testing

Wear testing was initiated on boar cartilage specimens within 3-5 hours of death.

Throughout testing, each cartilage specimen was immersed in 5 mL of culture media made primarily of Dulbecco's Modified Eagle Medium (DMEM), a cell culture medium, with 10% fetal bovine calf serum (ACS; GE Healthcare Life Sciences, Utah, USA). The media solution also contained 1% Penicillin-streptomycin antibacterial and 1% Amphotericin B anti-fungal reagents to prevent contamination during testing. This culture medium solution provides nutrition and lubrication simultaneously<sup>98</sup>. Fetal bovine calf serum has similar protein constituent fractions to synovial fluid<sup>106</sup>.

Specimens were randomly assigned to the five RoC treatment groups and control group. Treatment groups were cycled using a six-station pin-on-plate wear simulator in linear reciprocal sliding (Figure 2-4 and Figure 2-5). A constant load of 27.5 N was applied to each pin as it slid against the cartilage surface for 10,000 cycles at a frequency of 1.2Hz and 10 mm stroke length. This duration of testing (140 minutes) was deemed appropriate because all cartilage specimens displayed visible wear tracks after testing yet had not been worn down to the underlying subchondral bone. A previous study in the lab demonstrated that the 27.5 N load produces stress levels in the cartilage within a clinically relevant range for numerous hemiarthroplasty implant procedures<sup>10</sup>. Wear testing was performed at room temperature ( $25\pm 1^{\circ}\text{C}$ ).

The control group specimens were treated the same as the test specimens, without being worn by an implant pin. Control cartilage specimens were harvested, submerged in 5mL of the DMEM solution, and left untouched for the allotted time.



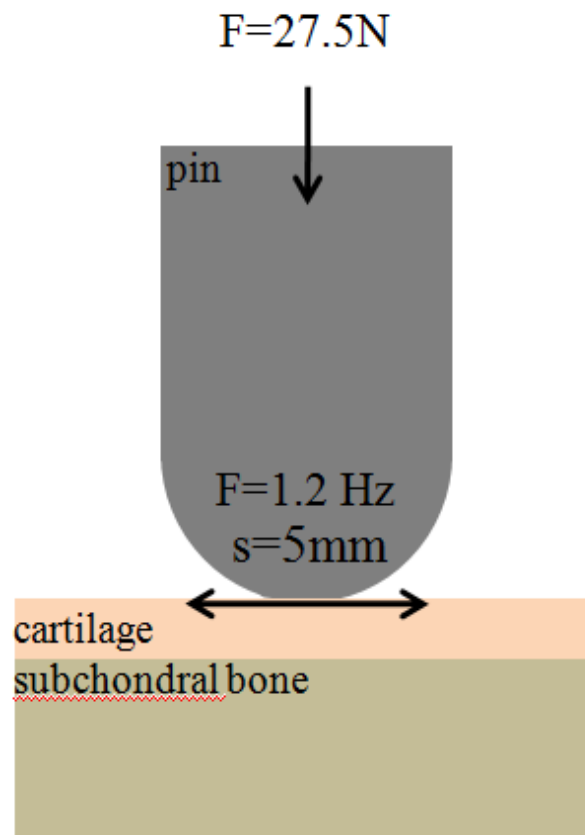


**Figure 2-3:** *The specifics of the testing set up of the pin-on-plate wear simulator against cartilage specimens.*

*A constant load of 27.5 N was applied down on each of the five pins in linear reciprocal sliding against the articular cartilage surface. Frequency = 1.2 Hz, Stroke length (s) = 5 mm.*



**Figure 2-4:** *Wear testing set up.*

*The testing setup of the six-station pin-on-plate wear simulator, stainless steel implant pins, and cartilage specimens submerged in culture media.*

### 2.2.3 Post-wear Analyses

Within each RoC treatment group and the control group there were two different treatment protocols (Figure 2-6):

- Treatment protocol 1: six (6) cartilage specimens were randomly assigned to each RoC/control group, where they underwent wear testing and then were submerged in the culture media in 10% carbon dioxide at 37°C for **24 hours**.
- Treatment protocol 2: six (6) cartilage specimens were randomly assigned to each RoC/control group, where they underwent wear testing and then were submerged in the culture media in 10% carbon dioxide at 37°C for **72 hours**.

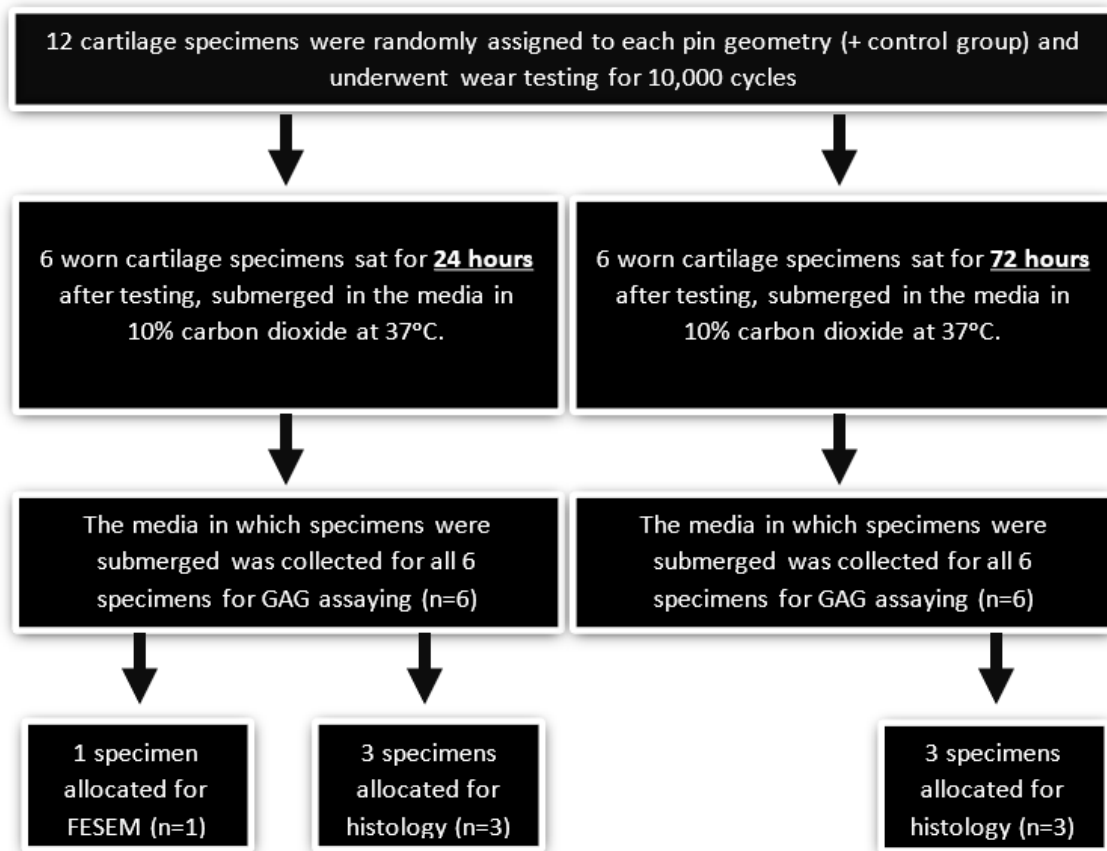


**Figure 2-5:** A summary of treatment allocations for the worn cartilage specimens.

*A flow chart demonstrating treatment allocations of all cartilage specimens for GAG assaying, histology, and field emission scanning electron microscopy (FESEM) at 24- and 72-hour time points.*

After wear testing, worn and control specimens were placed in a tissue incubator at 10% carbon dioxide at 37°C for 24 (n=6) or 72 hours (n=6) submerged in the DMEM solution. This environment aids in regular cell activity for mammalian cells which requires slightly acidic conditions. After the specimen's allotted time, the DMEM solution was collected for sGAG assaying, and the specimens were harvested for histology and surface morphology analysis.

The time points of 24 and 72 hours were chosen for this study based on pilot studies assessing changes in proteoglycan concentration 0, 12, and 24 hours after wear (Appendix

B), as well as literature indications that cell cultures of 72 hours have increased GAG concentrations relative to those at 24 hours<sup>107</sup>.

## 2.2.4 Assays

### 2.2.4.1 Proteoglycan Assay

A 1 mL aliquot of the culture media was allocated for proteoglycan quantification for each of the six cartilage specimens soaked for 24 hours, and for each of the six specimens soaked for 72 hours.

A Blyscan sGAG Assay Kit<sup>108</sup> was used to determine proteoglycan concentrations in the DMEM solution in which the cartilage samples were submerged during testing to assess proteoglycan release from the cartilage. This assay uses 1,4-dimethylmethylene blue dye to colorimetrically quantify sGAG content. Pilot studies determined optimal concentration of the samples and the amount of time the cartilage should soak in the cell culture solution (Appendix B).

Following wear testing, the cartilage remained fully submerged in the media for 24 hours or 72 hours in a tissue culture incubator with an environment of 10% carbon dioxide at 37°C. After the set time, 1 mL aliquots of the pooled DMEM culture media solution were collected from each sample for proteoglycan quantification. Aliquots were frozen at -80°C and then concentrated approximately 8-fold from 0.8 mL to ~0.1 mL using a CentriVap Centrifugal Concentrator. The aliquots were concentrated this amount to ensure points fell along the generated calibration curve (Figure 1-6) and yielded accurate results as determined by pilot studies in which different concentrations were tested (Appendix B). A media blank and deionised water blank were also assayed for GAG concentration as test controls.

The Blyscan sGAG Assay Kit protocol was followed<sup>109</sup>. GAG standards were prepared with deionised water and 1.0, 2.0, 3.0, 4.0, and 5.0 µg of the reference standard – a sterile solution of bovine tracheal chondroitin 4-sulfate (100 µg/mL). 1.0 mL of GAG dye reagent was added to each sample and mixed using a mechanical shaker for 30 minutes. After this

time, a sGAG-dye complex precipitated. The microcentrifuge tubes were then centrifuged at 13,000  $xg$  for 10 minutes to collect the precipitate and pack it at the bottom of each tube. All unbound dye was drained from the tubes, leaving just the precipitate. 0.5 mL of a dissociation reagent was added to each tube to release the bound dye into solution and samples were then centrifuged again for 5 minutes to remove foam before being transferred to individual wells of a 96 micro well plate. Each sample was entered in duplicate. A Biotek™ Eon™ microplate spectrophotometer was used to measure the absorbance of resulting samples, deionised water blank, media blank, and standards (0.1-0.5  $\mu g$ ) at a wavelength of 656 nm. A calibration curve (Figure 2-7) was constructed using the standard absorbances and their known concentrations, and sample concentrations were calculated from the absorbance using the linear trendline equation. Sample absorbances were corrected by subtracting the y-intercept – the absorbance detected at 0  $\mu g/mL$  proteoglycan concentration.

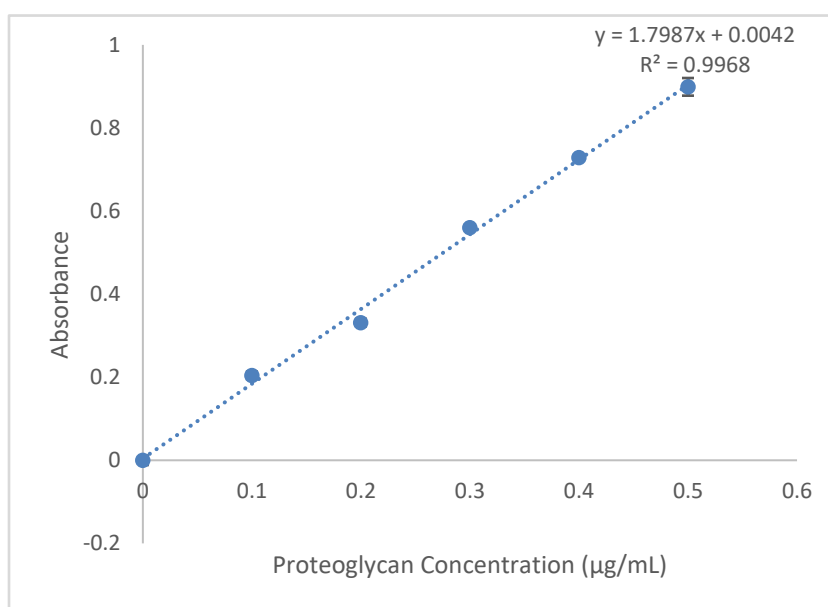


**Figure 2-6:** Calibration curve for calculating proteoglycan concentrations.

A calibration curve ( $y = 1.7987x + 0.0042$ ,  $R^2 = 0.9968$ ) constructed using known proteoglycan concentrations of 0.1, 0.2, 0.3, 0.4, and 0.5  $\mu g/mL$ . Standard deviation error bars are shown. The absorbance was measured at a wavelength of 656nm using a microplate reader.

The mean values for treatment groups were statistically compared ( $\alpha=0.05$ ) using a one-way ANOVA and followed by a Tukey multiple comparison test, both using IBM® SPSS® Statistics Software.

#### 2.2.4.2 Histology

Three cartilage specimens soaked for 24 hours, and three specimens soaked for 72 hours were allocated for histological assessment.

Histology blocks were harvested from the center of the cartilage specimens and perpendicular to the wear track. After harvesting, the samples were fixed in 10% formalin to preserve and stabilize the tissue. The samples then underwent decalcification, embedding, sectioning, and staining at the Molecular Pathology Core Facility at Robarts Research Institute (Western University, London, ON). The embedding replaced the water content of the cartilage tissue with solidifying paraffin. The paraffin blocks were positioned for cross-sectional view of the cartilage, with the cartilage surface facing up. A microtome then sliced five (5)  $\mu\text{m}$  sections at different depths throughout the cartilage paraffin blocks, and a total of 10 sections were taken per sample. All sections were stained using Safranin-O/Fast Green to show proteoglycan concentration within the tissue, cell distribution, and surface condition<sup>110,111</sup>. Safranin O stains sGAGs and is proportional to the proteoglycan content in cartilage, and the Fast Green counterstains for contrast.

Slides were scanned using an Aperio AT2 system (Leica Biosystems, Wetzlar, Germany). Cartilage specimens were assessed qualitatively at 4x magnification and based on cartilage surface intactness and smoothness, organization of the cells, and concentration of the stain showing proteoglycan concentration and distribution.

#### 2.2.4.3 Surface Morphology

For each pin geometry and the control group, one cartilage specimen underwent surface morphology analysis to complement the above-mentioned biological assays.

Cartilage specimens were examined via FESEM at 200x and 1000x to assess surface morphology. A small cubic section ( $\sim 5 \times 5 \times 5$  mm) was harvested from the center of the

wear track on each cartilage specimen, thoroughly rinsed with deionised water, and immediately soaked in 100% ethanol. Samples were prepared for FESEM with critical point drying since water molecules interfere with the vacuum in the field emission scanning electron microscope. This is an effective method of drying delicate samples while preserving and protecting the surface from potential damage caused by surface tension during evaporation<sup>112</sup>.

The specimens underwent critical point drying to preserve the three-dimensional structure of the samples. FESEM imaging at the Western Nanofabrication Facility (Western University, London, ON). A Zeiss 1540XB field emission scanning electron microscope (Zeiss, Oberkochen, Germany) was used for imaging.

Cartilage surface condition was assessed qualitatively by shape, size, and number of undulations, as well as identification of any irregularities and fissures.

#### 2.2.4.4 Summary

To summarize, key outcome metrics related to the biological response of cartilage to hemiarthroplasty implant curvature were assessed using proteoglycan assay, histology, and surface morphology. A Blyscan sGAG Assay Kit<sup>108</sup> quantified proteoglycan released from cartilage specimens at 24 and 72 hours after wear testing. Histology slides stained with Safranin O/Fast Green were qualitatively assessed at 24 and 72 hours after wear via surface condition, cell organization, and proteoglycan distribution. Lastly, surface morphology was captured using FESEM and qualitatively assessed by surface condition, appearance of undulations, and other irregularities identified when compared to the control specimen.

## Chapter 3

### 3 Results

*Overview: This chapter presents the results of the outlined studies investigating the effect of metal implant curvature on early biological markers of cartilage wear. Results include measurement of proteoglycan release into the pooled culture media in which cartilage specimens were submerged after testing for 24 (n=6) or 72 hours (n=6); histology images (x4 magnification) of cartilage specimens 24 (n=3) or 72 hours (n=3) after wear; and field emission scanning electron microscopy (x1000 magnification) images (n=1) showing cartilage surface morphologies after wear.*

#### 3.1 General Observations

Testing was uneventful and followed the planned methodologies. The radiocarpal joints obtained from the abattoir appeared healthy when harvested and the cartilage had no visible surface damage prior to the wear testing.

All pin geometries investigated produced visible wear tracks on the cartilage surface. A typical wear track is shown in Figure 3-1.



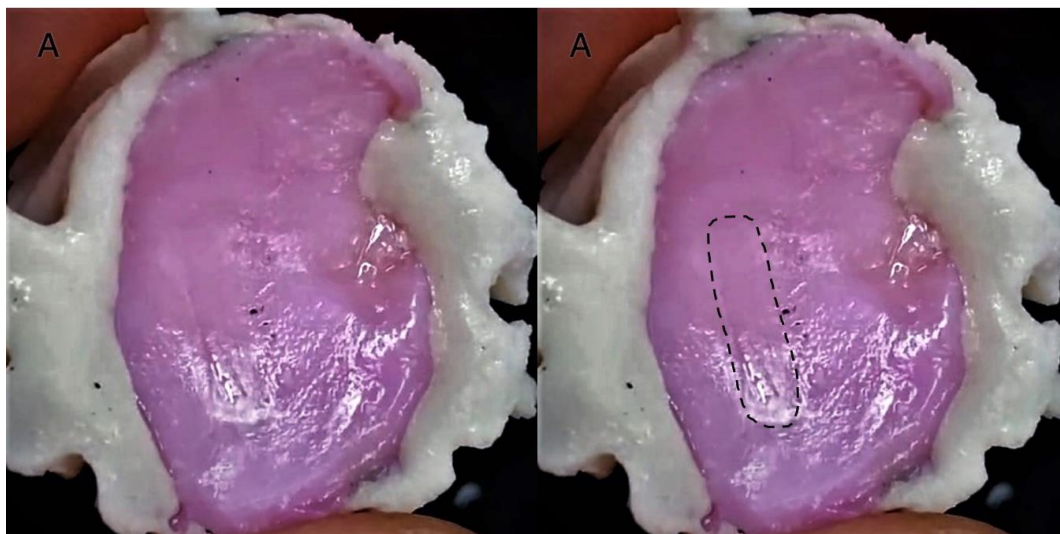


**Figure 3-1:** A typical wear track on a worn cartilage specimen.

*An example of the wear tracks seen after wear testing is shown. The image is duplicated (left) showing a raw image of a cartilage specimen and its resulting wear track and (right) showing the wear track digitally outlined. There were no visible differences in wear tracks observed across treatment groups. The cartilage appears pink from being submerged in the DMEM culture media, which is a pink solution.*

## 3.2 Proteoglycan Assay

Figure 3-2 shows the resulting mean proteoglycan concentration in the medium representative of  $n=6$  for each pin geometry and the control at 24 hours after wear testing. A one-way ANOVA determined that there was no significant difference in proteoglycan concentration between the treatment groups ( $p>0.05$ ) (Figure 3-2). There was no significant difference in the average proteoglycan concentration resulting from the different pin geometries (4.70-11.70 mm) ( $p>0.05$ ). The pin geometries investigated did not result in significantly different proteoglycan concentrations relative to the unworn control specimens ( $p>0.05$ ).

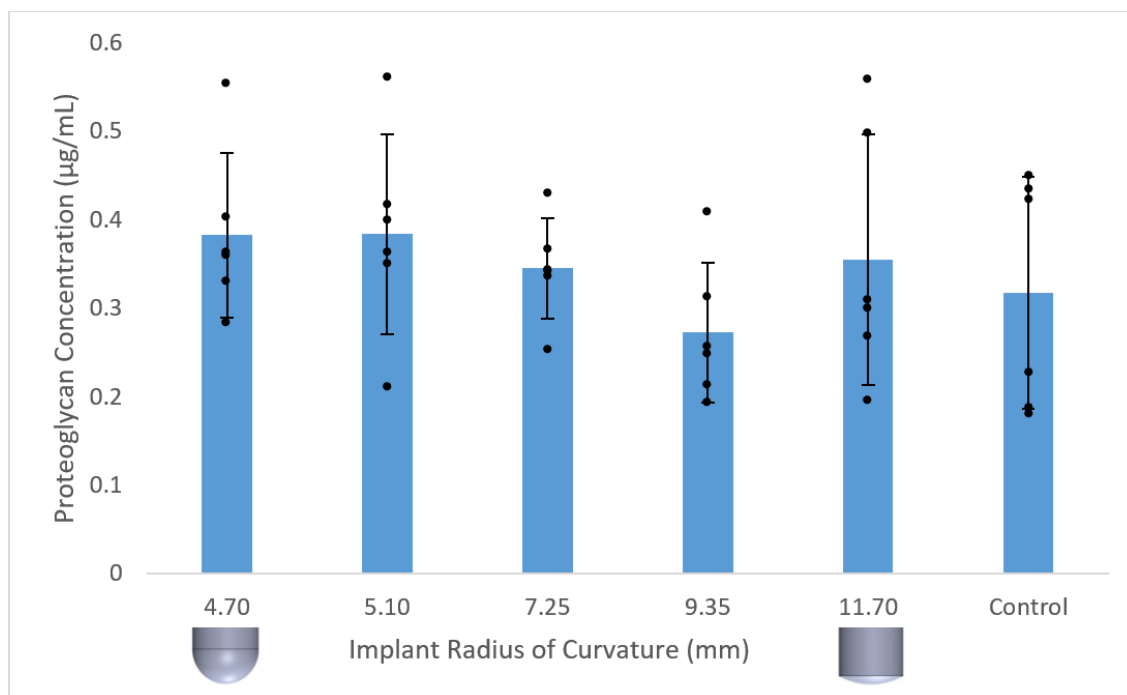


**Figure 3-2:** Plot of average proteoglycan concentration 24 hours after wear testing for each implant radius of curvature (RoC) treatment group.

The mean  $\pm$  standard deviation proteoglycan concentration released from cartilage specimens into the culture media for each corresponding RoC treatment group ( $n=6$ ) after 24 hours in 10%  $CO_2$  and 37°C. Individual data points are also included for each treatment group. No significant differences were present between groups ( $p<0.05$ ).

Figure 3-3 shows the resulting mean proteoglycan concentration in the medium representative of  $n=6$  for each pin geometry and the control at 72 hours after wear testing. A one-way ANOVA determined that there were statistically significant differences between the means of treatment groups ( $p<0.05$ ) (Figure 3-3). The results showed increased proteoglycan release from cartilage specimens worn with stainless steel pin geometries (4.70-11.70 mm) compared to unworn cartilage specimens. All pin geometry treatment groups resulted in a greater average proteoglycan concentration than in the control group, although not all effects were statistically significant.

Proteoglycan concentration resulting from wear with the 4.70 mm and 9.35 mm pins were significantly greater than in the control ( $p=0.04$  and 0.02, respectively).

There were no significant differences between the proteoglycan concentrations resulting from pin geometries 4.70-11.70 mm ( $p > 0.05$ ).

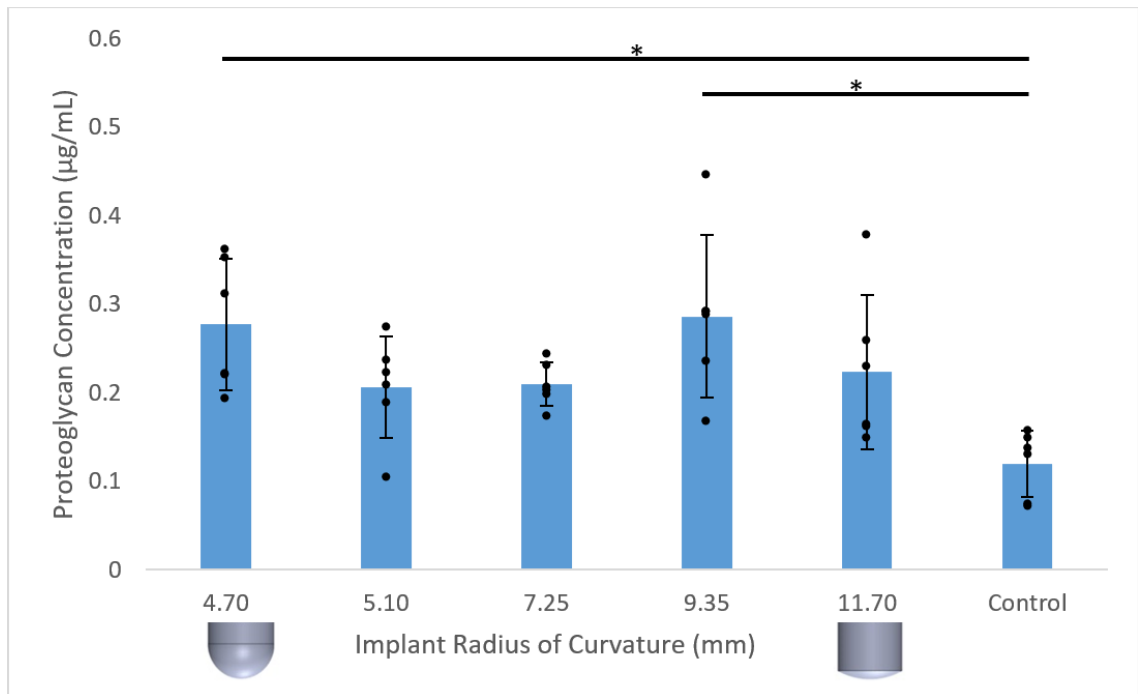


**Figure 3-3:** Plot of average proteoglycan concentration 72 hours after wear testing for each implant radius of curvature (RoC) treatment group.

The mean  $\pm$  standard deviation proteoglycan concentration released from cartilage specimens into the culture media for each corresponding RoC treatment group ( $n = 6$ ) after 72 hours in 10%  $CO_2$  and 37°C. Individual data points are also included for each treatment group. RoC 4.70 mm and 9.35 mm resulted in significantly greater proteoglycan concentrations than the control group ( $p = 0.04$  and 0.02, respectively). (\*  $p < 0.05$ ).

### 3.3 Histology

The histological analysis of cartilage specimens 24 hours after wear testing showed no differences between cartilage specimens worn by different stainless steel pin geometries (4.70-11.70 mm), as well as compared to the control. All cartilage specimens appeared healthy, with an intact surface and no differences in proteoglycan concentration or distribution were observed. There were four visible zones in which the matrix and chondrocytes were organized, and there were no apparent differences in cell count.

Figure 3-4 shows histology images representative of n=3 taken 24 hours after wear testing for each pin geometry (4.70-11.70 mm) (a-e) and the control (f). Histology images representing pin geometries 4.70, 5.10, 7.25, and 11.70 mm (a, b, c, and e) show an intact surface with no irregularities and the cartilage morphology is intact with normal architecture, and appropriately oriented cells. The 9.35 mm pin (d) resulted in a lighter, decreased staining than other pin geometries; however, this is likely due to differences in histological preparation/staining and not a difference in proteoglycan concentration caused by wear as there are no other signs of cartilage damage – there is an intact surface, and intact cartilage morphology. The control specimen (f) represents healthy unworn cartilage, with intact cells and cartilage morphology.

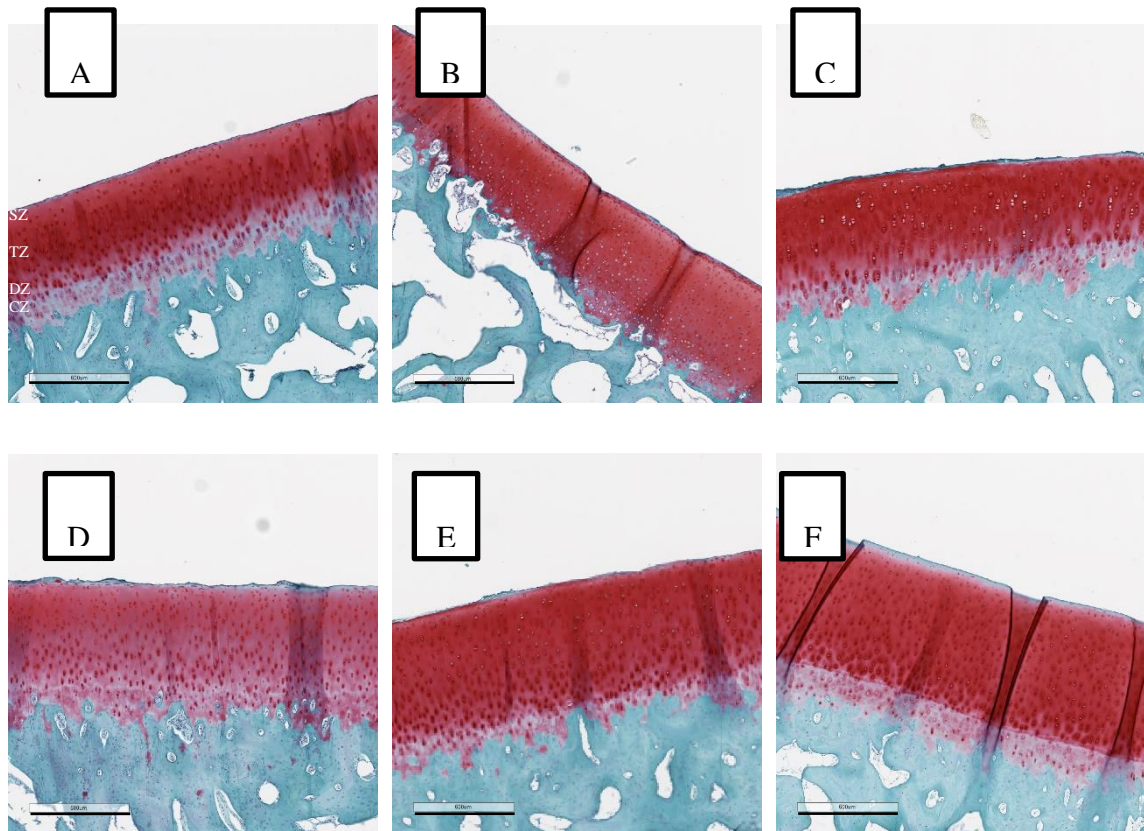


**Figure 3-4:** Histology images ( $n=3$ ) of cartilage specimens 24 hours after wear with different pin geometry's and stained with Safranin-O/Fast Green.

Pin geometries **A)** 4.70 mm, **B)** 5.10 mm, **C)** 7.25 mm, **D)** 9.35 mm, **E)** 11.70 mm, and the unworn control specimen (**F**). Images are representative of  $n=3$  cartilage specimens. Cartilage cross-sections are shown at  $\times 4.0$  magnification. The scale bar in the bottom left corner of each image shows 600  $\mu\text{m}$ . Roberts Research Institute Facilities (Western University, London, ON). The four zones of articular cartilage are labelled on A. SZ, superficial zone; TZ, transitional zone; DZ, deep zone; CZ, calcified zone.

Cartilage specimens left in the culture media for 72 hours after wear testing showed no differences in surface condition, cartilage morphology, and proteoglycan concentration between cartilage specimens worn by pin geometries (4.70-11.70 mm), and also compared to the control. All cartilage specimens had an intact surface, intact cartilage morphology, and regular proteoglycan distribution. There were four visible zones in which the matrix and chondrocytes were organized and there were no apparent differences in cell count.

Figure 3-5 shows histology images representative of  $n=3$  taken 72 hours after wear, for each pin geometry (4.70-11.70 mm) (a-e) and the control (f). Histology images representing pin geometries 4.70-11.70 mm (a-f) show an intact, smooth surface and intact cartilage morphology with normal architecture, and appropriately oriented cells. The intensity of the Safranin-O/Fast Green staining shows there were no differences in proteoglycan concentration and distribution across the five RoC treatment groups and compared to the control.

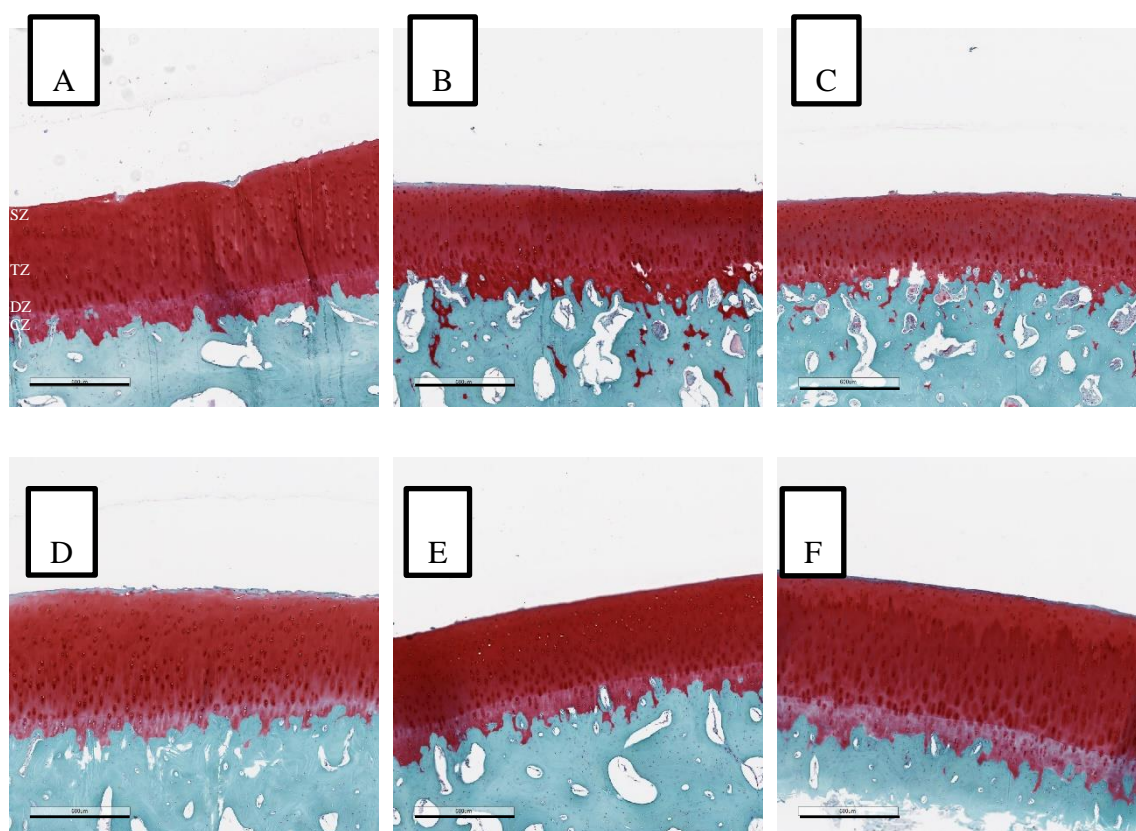


**Figure 3-5:** *Histology images ( $n=3$ ) of cartilage Specimens 72 hours after wear with different pin geometry's and stained with Safranin-O/Fast Green.*

*Pin geometries A) 4.70 mm, B) 5.10 mm, C) 7.25 mm, D) 9.35 mm, E) 11.70 mm, and the unworn control specimen (F). Images are representative of  $n=3$  cartilage specimens. Cartilage cross-sections are shown at  $\times 4.0$  magnification. The scale bar in the bottom left corner of each image shows  $600\ \mu\text{m}$ . Robarts Research Institute Facilities (Western University, London, ON). The four zones of articular cartilage are labelled on A. SZ, superficial zone; TZ, transitional zone; DZ, deep zone; CZ, calcified zone.*

### 3.4 Surface Morphology

Cartilage surface morphology showed differing amounts of damage resulting from the different pin geometries and compared to the control specimen under FESEM. Cartilage surfaces worn with pin geometries 4.70-11.70 mm resulted in increasing damage with decreasing RoC (n=1).

It is evident in Figure 3-6 that the (a) 4.70 mm RoC pin caused the most surface damage to the cartilage as there are major surface irregularities and fibrillations with sharp ridges characterized by wide and deep valleys. Pins (b-d) 5.10-9.35 mm resulted in an uneven surface filled with undulations. However, in the sequential order of (b-d) 5.10-9.35 mm there is a decrease in the number of undulations and the undulations become more rounded, indicating decreasing damage. Finally, the (e) 11.70 mm pin resulted in a smooth and even surface with striations, representing the least cartilage surface damage. The unworn control specimen (f) shows an even and smooth surface with small loose fissures, representing natural texture of a native cartilage surface.

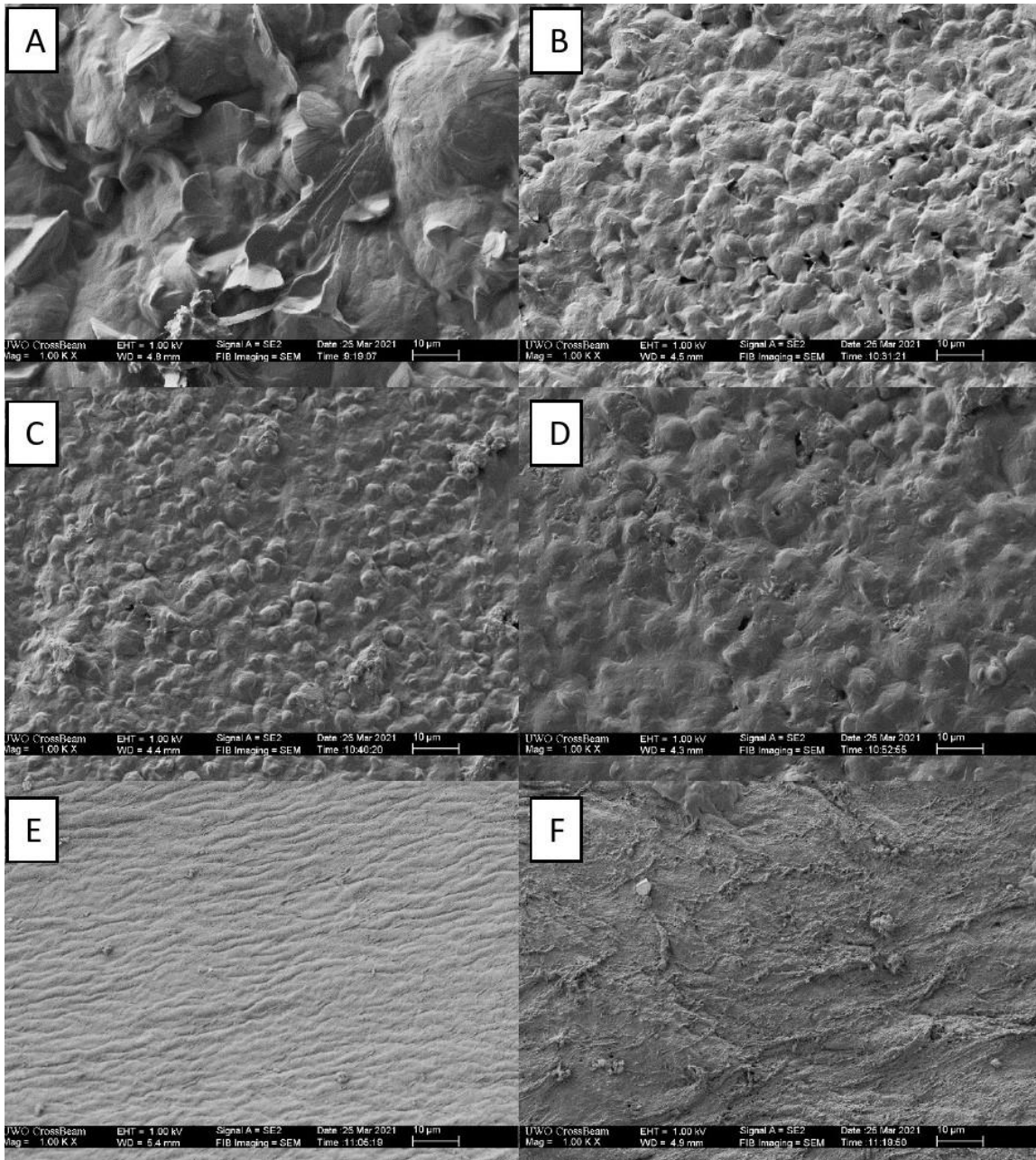


**Figure 3-6:** Field emission scanning electron microscopy images of cartilage surfaces worn with different pin geometries.

Pin geometries **a)** 4.70 mm, **b)** 5.10 mm, **c)** 7.25 mm, **d)** 9.35 mm, **e)** 11.70 mm, and the unworn control specimen **(f)**. Cartilage surfaces are shown at  $\times 1000$  magnification. The scale bar in the bottom right corner of each image shows  $10\ \mu\text{m}$ . Western Nanofabrication Facility (Western University, London, ON).



### 3.5 Summary

Overall, proteoglycan assay results showed increased proteoglycan release from cartilage specimens worn with metal (stainless-steel) implant pins of various geometries (4.70-11.70 mm) compared to unworn control cartilage specimens after 72 hours but not 24 hours. However, there was no significant difference in proteoglycan release between the five different implant curvatures. Histological analysis appeared to show no differences between treatment groups as all cartilage specimens appeared healthy with no signs of damage. Results from FESEM showed increasing cartilage surface damage with decreasing implant RoC. These findings are discussed in the next chapter (Chapter 4).

## Chapter 4

### 4 Discussion

*Overview: This chapter discusses the research findings reported in the Results (Chapter 3) and explores the principal findings, possible implications, and overall relationship to previous literature. It covers limitations of the research as well as future directions. The importance of the findings is analyzed, and final conclusions are presented.*

#### 4.1 Principal Findings

The purpose of this research was to investigate the early biological responses of articular cartilage worn by five different hemiarthroplasty metal (stainless steel) implant curvatures through measurement of proteoglycan release, histological analysis, and FESEM analysis. It was also to compare the cartilage biological responses at 24 hours and 72 hours after wear testing.

While only the pin geometries of 4.70 mm and 9.35 mm caused a statistically significant difference from the control ( $p=0.04$  and  $0.02$ , respectively) after 72 hours, all the pin geometries resulted in greater average proteoglycan release into the pooled culture media than the control. There were no differences in proteoglycan concentrations reported at 24 hours after wear testing. An increase in proteoglycan concentration in the pooled culture media represents increased proteoglycan release from the cartilage. Thus, proteoglycan release from the cartilage had a delayed response as there was increased proteoglycan release from the cartilage specimens worn with the pin geometries (4.70-11.70 mm) compared to the unworn control specimens at 72 hours but not at 24 hours after wear testing. However, there were no significant differences in proteoglycan release between the different pin geometries at both 24 and 72 hours after wear. This data suggests that proteoglycan release may not be an immediate response to mechanical wear, but rather is secondary to increased expression of proteases such as matrix MMPs and ADAMTSs. Expression and/or activation of these proteases might be an induced response to loading

and could result in breakdown of the ECM, including proteoglycans. These results suggest that there appears to be a delayed biological response to early wear of 72 hours.

The histology images showed no indications of structural damage to any cartilage specimens and no differences in proteoglycan distribution/concentration at 24 and 72 hours after wear. All specimens had intact surfaces and intact cartilage morphology. This contrasts with what was observed biochemically in the quantitative proteoglycan assay. The probable reasoning for this is that proteoglycan release quantified in the GAG assay was slow and subtle and hence was not visible in a less sensitive and less quantitative assay, such as histological staining. It is expected that histology would reflect damage only after a greater substantial loss of proteoglycans, which would more likely occur after an extended period of wear testing and perhaps under more extreme loading conditions. Additionally, it was observed that some of the histology images exhibit differences in the thickness of the cartilage (stained red), which can be an indicator of wear as well. However, this is not believed to be an indicator of wear for this histology study but more likely a result of angular differences in which slides were sectioned. Boar specimens used were male and similar in age and weight, and so specimens are expected to have similar starting cartilage thickness prior to testing. For wear to affect the thickness of cartilage, a much longer period of wear testing would be required as this is used in assessing progression of OA<sup>113-115</sup>. This study focuses primarily on early cartilage wear to understand the early biological responses of cartilage to joint hemiarthroplasty. These histological findings have confirmed that the hemiarthroplasty devices employed and the testing methodology do not cause sufficient damage to be visible in histology assays, likely due to cartilage's abilities to withstand loading.

Regarding the GAG assay, the proteoglycan release measured from control specimens represents the natural turnover of unloaded cartilage, without aggressive wear or damage. The increased proteoglycan release from the cartilage specimens worn with the hemiarthroplasty implant pins (4.70-11.70 mm) is indicative of the breakdown of the ECM and catabolic cellular responses to damage caused by the metal implant pins. Chondrocytes synthesize and turnover proteoglycans for regular function of the cartilage, but also in response to damage or inflammation<sup>8,61,116,117</sup>. It is known that the MMP and ADAMTS

enzyme families actively degrade proteoglycans, particularly aggrecan, in response to cartilage damage and that this degradation is associated with the progression of OA and rheumatoid arthritis<sup>84,87,118,119</sup>. Such degradation of proteoglycans directly affects cartilage function, for example, aggrecan gives cartilage its compressive load-bearing properties. Thus, significant degradation by MMPs and ADAMTSs may make the cartilage more susceptible to further damage under loading<sup>117,120,121</sup>.

Schätti et al. developed a model to study mechanical and biological responses of articular cartilage to sliding loads<sup>122</sup>. The research investigated the effect of axial loads on gene expression of anabolic and catabolic proteins. The catabolic proteins included MMP-13, ADAMTS-4, and ADAMTS-5. The results found a correlation between increasing both strain and contact stress and increased gene expression of the above-mentioned proteases. Another study by Lee et al. examined the time-dependent changes in chondrocyte gene expression resulting from mechanical injury of cartilage explants<sup>123</sup>. An increase in MMP-3 and ADAMTS-5 expression was recorded after injury was induced by compression of free swelling cartilage and was time-dependent. MMP-3 gene expression increased until the 12-hour mark and then decreased, and ADAMTS-5 showed a similar trend as well. Wang et al. recorded that inhibited activity of MMP-13 in mice decelerated OA progression<sup>118</sup>. Double-knockout of ADAMTS-4 and ADAMTS-5 genes in mice in a study by Majumdar et al. significantly reduced proteoglycan degradation and the progression of OA<sup>119</sup>. These studies highlight the probable cause of the increased proteoglycan release from worn cartilage specimens as reported in our results after 72 hours. Since the boar specimens underwent wear testing within 3-5 hours of slaughter, the chondrocytes and enzymes were expected to be functioning and responsive to cartilage damage, and the biochemical activity identified in our study is supportive of that model. Increased proteoglycan release into the culture media in which cartilage specimens were submerged is suggestive of proteoglycan degradation and ECM breakdown in response to the wear testing. This could be due to increased catabolic processes such as activation of MMP-13, ADAMTS-4, and ADAMTS-5 to actively degrade proteoglycans. Since proteoglycan degradation is secondary to the over-expression of these enzymes, this is supportive of the delayed response of 72 hours after wear testing.

Wear with metal implant pin models caused a biological response in cartilage 72 hours after the wear testing, but at this stage of early wear there was no effect of implant curvature on the biological response of cartilage. It is known that more conforming geometries of hemiarthroplasty implants reduce contact stresses, wear, and may improve longevity<sup>10,124-127</sup>. There are many other variables affected by implant curvature. McCann et al. studied the effect of conformity of knee hemiarthroplasty implant designs on contact stress, friction, and degeneration of articular cartilage<sup>76</sup>. A decrease in RoC resulted in an increase in contact stress, coefficient of friction, friction shear stress, and cartilage degeneration. Lizhang et al. found that decreasing RoC of cartilage pins worn against cobalt chromium alloy (CoCr) plates resulted in increasing coefficients of friction in early cartilage wear<sup>21</sup>.

A similar study by Khayat investigated the relationship between the contact area of metal pins and the wear they induced on articular cartilage<sup>10</sup>. The loading conditions, number of wear testing cycles, and metal pin curvatures tested were the same as in our current study. The study quantified volumetric wear and wear depth using 3D contact scanners and it was reported that increased contact area resulted in decreased cartilage wear. The data suggests that when load is distributed over a greater area, less acute cartilage damage occurs. This is likely attributed to the improved contact mechanics resulting from an increased RoC. Contact stresses were measured using a pressure-sensitive Fuji Film for each implant geometry in this study, and they ranged from 1.42 MPa in the 11.70 mm pin to 2.84 MPa in the 4.70 mm pin<sup>10</sup>. As radius of curvature decreases, the resulting wear track width decreases, and thus contact stresses between the implant and cartilage increases. With increased wear times or more aggressive wear it is expected that decreasing wear track width and increasing contact stresses would result in increasing proteoglycan release.

While those results showed that a more conforming pin geometry may reduce cartilage wear, our study demonstrated no effect of pin geometry on biological markers of cartilage wear. This may imply that early markers of cartilage wear are primarily mechanical, especially since the proteoglycan release caused by wear was delayed to 72 hours. Considering these mechanical responses to implant curvature, it could be expected that a

biological response to implant curvature would be observed with increased wear time or more aggressive wear.

Our FESEM findings support the macroscopic wear findings by Khayat. With the caveat that it was a sample size of one, the FESEM results agree with the results of Khayat's *in vitro* study as the images showed decreasing damage to the cartilage surface with increasing RoC of the implant model. The trend did not appear to be linear as the implant RoC's 5.10-9.35 mm showed similar wear mechanisms but with a steady decrease in surface damage as the number of undulations decreased and the undulations became more rounded. However, the RoC 4.70 mm resulted in a different pattern completely, with the major surface fibrillations and sharp ridges indicating more aggressive damage and possible tearing. On the other end of the spectrum, the 11.70 mm pin also exhibited a unique pattern, but one that was flat and smooth with striations. Even though the 11.70 mm pin resulted in no indications of surface damage as deemed by surface morphology, differences were still noted when compared to the control. In fact, the surface appeared 'smoother' than the control. A plausible explanation for this could be that the 11.70 mm pin is smoothening the natural texture seen on the native cartilage surface without damaging the surface. This may indicate that wear mechanisms first act to flatten and smoothen a cartilage surface before causing damage. This implies that there could be critical point after which the RoC becomes significantly detrimental to the cartilage. Interestingly, Khayat's wear study also suggested a 'threshold' at which cartilage sensitivity to RoC shifts<sup>10</sup>.

Graindorge et al. studied sheep knee joints worn in a joint simulator for different periods of time and assessed changes in cartilage surface morphology and wear particle morphology<sup>100</sup>. Their SEM and environmental-SEM (ESEM) images revealed increasing surface damage with increasing duration of wear testing. This study simulated the normal walking cycle of a sheep joint for 10, 15, 20, 30, and 45 minutes and so had shorter wear times compared to our 140-minute wear study. A cartilage-on-cartilage wear study by Verberne et al. investigated surface morphology of human articular cartilage using an optical microscope<sup>78</sup>. They shared an image (included below as Figure 4-1) capturing the boundary between a worn and unworn area on the cartilage surface after wear testing of

300,000 cycles under a load of 60 N. Figure 4-2 is also included to compare our FESEM results of RoC's 5.10-9.35 mm and the control group. Verberne et al.'s results showed clear surface damage to the worn area with bowl-shaped depressions (Figure 4-1) similar in appearance to the undulations observed in our FESEM results for (b-d) RoC's 5.10-9.35 mm (Figure 4-2). In addition, the unworn section in Figure 4-1 is smooth and devoid of any morphological features, which corresponds to our (f) unworn control FESEM image in Figure 4-2. It is necessary to note that Figure 4-1 and Figure 4-2 are not directly comparable as Verberne et al.'s study is cartilage-on-cartilage and uses human articular cartilage from donor's aged 70-85 years old, and there is a difference in scale, methodologies, and wear testing times; however, it is important to highlight the similarity in textures which reinforces the patterns of wear observed in our study. The parallels between our results could imply validity and repeatability for our FESEM results.

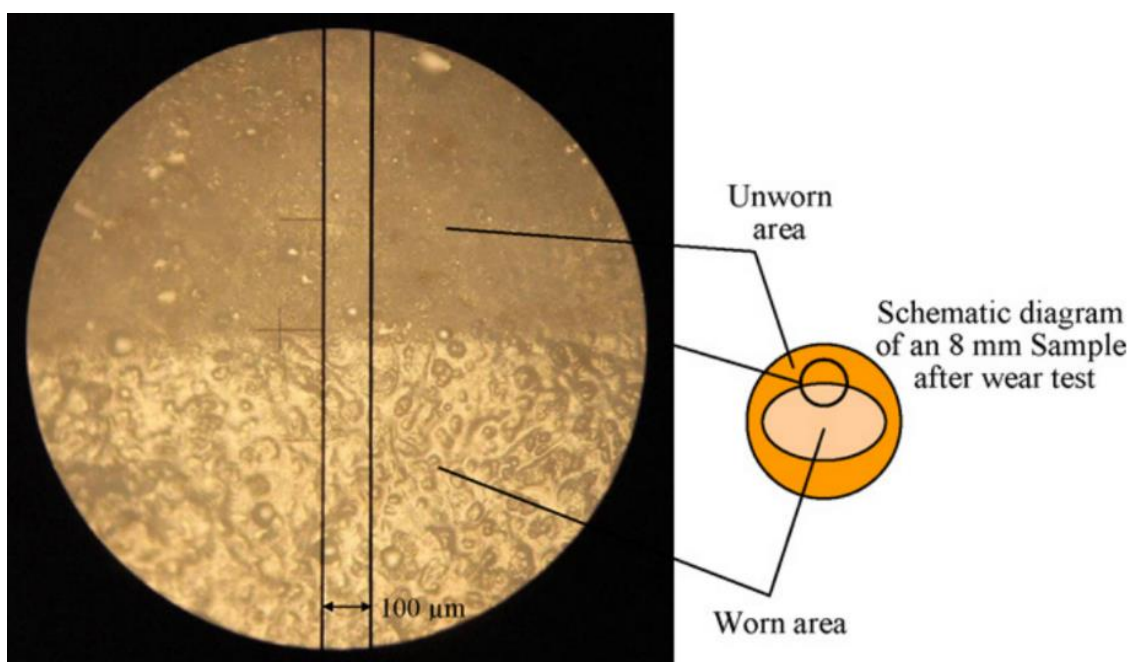


**Figure 4-1:** Photograph from Verberne et al. capturing the boundary of a wear track on the cartilage surface<sup>78</sup>.

Figure taken from Verberne et al.<sup>78</sup>. A worn area and unworn area are shown and labelled on an 8 mm diameter cartilage specimen after 300,000 cycles of 60 N loaded cartilage-on-cartilage wear testing. Image was captured using optical microscopy. A scale bar of 100  $\mu\text{m}$  is shown.

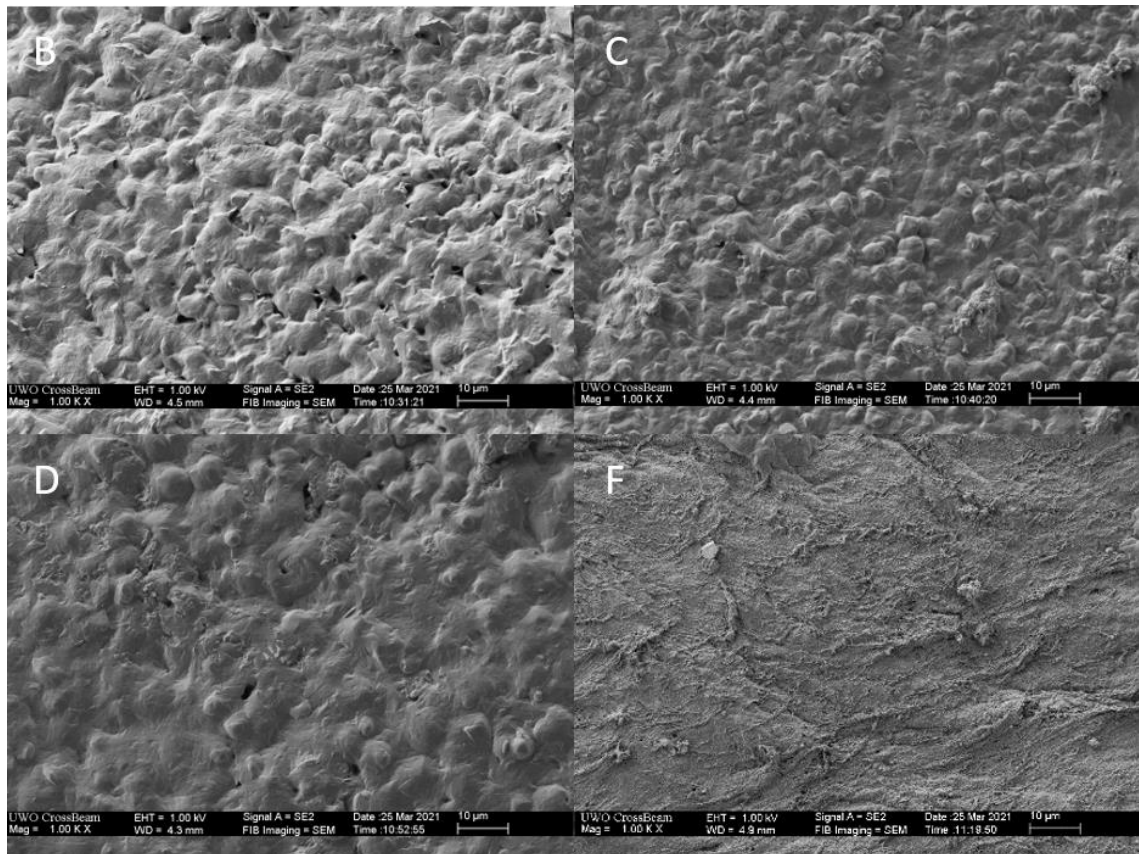


**Figure 4-2:** FESEM images of cartilage surfaces worn with (B-D) 5.10-9.35 mm pins respectively and the unworn (F) control.

*Repeated images from the FESEM results (Chapter 3.3) section in order to draw parallels with other studies.*

Some differences between the FESEM and histological assay were noted in the current study. The surface morphologies indicating damage in the FESEM were not observed in the histology images because of the difference in the magnification. The surface damage to the cartilage due to the hemiarthroplasty devices were subtle and only visible on a micro-scale. It is unknown if greater force and hence interface stresses had been applied or if longer wear studies had been performed if this micro damage would progress to become visible on standard histology. Further studies would be required.



Our observations are similar to a study by Cruess et al. who explored the *in vivo* response of articular cartilage to vitallium metal hemiarthroplasty prostheses over a total of 24 weeks in hips of dogs using SEM and histology<sup>53</sup>. With increasing time after operation there was increasing cartilage damage reported. Similar to the current *in vitro* study, Cruess et al. reported that at two weeks postoperatively the structural integrity of the articular cartilage was preserved on histology; however, proteoglycan loss was noted, and SEM identified frayed articular surfaces. At subsequent time intervals, Cruess et al. showed a progressive deterioration in cartilage resulting in OA. Unlike the current study, Cruess did not investigate different articular geometries, and this has not been reported by other authors to date.

## 4.2 Limitations

Some limitations of this study include the use of a pin-on-plate wear simulator. The wear simulator was used in linear reciprocal sliding which does not replicate native paths of motion, and the stainless-steel implant pins used were not polished to the same degree as commercial hemiarthroplasty implants. This could have resulted in increased damage to the cartilage, but this protocol was still considered suitable for this comparative study with the purpose of evaluating the effect of implant geometry on the biological responses of cartilage.

Another limitation is that *in vitro* studies may not replicate complex cellular responses that would occur *in vivo* since cells in isolated explants can behave differently than in their normal environment in a living organism<sup>128</sup>. For these reasons and to minimize such differences the wear testing was initiated within 3-5 hours of slaughter. An *in vitro* study establishing a live cartilage-on-cartilage interface for tribological testing by Trevino et al. assessed cell viability in steer cartilage specimens after three days of death when kept at 37°C and 5% carbon dioxide<sup>129</sup>. This study reported that tissue viability was maintained (>85% of cells remained alive) in free swelling cartilage, but there was increased cell death in the cartilage surface when articulated against metal for three hours/day for the three days. This could imply tissue viability for the current *in vitro* study, and that the majority of cell death is a biological response to wear by metal implants. Generally, *in vivo* and *in*

*vitro* cartilage study results in these short periods after death are not contradictory and *in vitro* studies give useful insights on *in vivo* cartilage activity<sup>130</sup>. Furthermore, our results are consistent with the *in-vivo* study of Cruess et al. supporting the relevance of our findings.

Swine specimens are commonly employed in medical research as they share many features in structure and composition with humans<sup>131,132</sup>. This research used healthy and mature male boar cartilage specimens. The literature suggests that mature cartilage is generally stiffer than immature cartilage so a similar investigation using immature cartilage may show more damage than observed in this study and may display more aggressive wear<sup>129,133–135</sup>. Hemiarthroplasty implants are clinically used in mature human adults and so testing with mature cartilage is more relevant to clinical applications. Females reportedly have thinner cartilage and lesser volume than males even when adjusted for body height and weight, and so our results apply specifically to males although the comparative trends investigated are not expected to be different in females<sup>136,137</sup>.

It is recognized that the resulting proteoglycan concentrations after 24 hours had greater absolute values overall compared to after 72 hours. The absolute values of proteoglycan concentration reported in our results are not comparable between the 24- and 72-hour time points, which is a limitation of the study. This is because the 24- and 72-hour samples were concentrated by approximately 8-fold using the CentriVap Centrifugal Concentrator but on different days. Concentrations were approximate and the end concentration was judged using eye-level comparison of sample volume to a 1mL sample and so is not consistent between time points. Samples of the same time points (24 hour or 72 hour) however, were concentrated to equal amounts as they underwent concentration at the same time, for the same duration, and were exposed to the same environment. If equipment allowed for the different time points to be conducted in one session or to a greater precision, it is expected that the absolute values of 72-hour samples would show greater proteoglycan content than the corresponding 24-hour samples.

A further limitation is that an unloaded control was used and not a cartilage-on-cartilage control. However, in normal physiological joint loading very little proteoglycan release is

expected and unloading of a joint can also be harmful to cartilage<sup>81</sup>. Trevino et al. established a live cartilage-on-cartilage interface for tribological testing and reported no difference in wear between cartilage-on-cartilage and unloaded controls as identified by proteoglycan release and histology<sup>129</sup>. In fact, McDonnell et al. tested specimens that had undergone 10 days of bed rest and found that when you remove loading from cartilage it increases aggrecan and cartilage turnover compared to normal physiological loading<sup>138</sup>. The removal of loading in this study is similar to the unloaded control used in our comparative study and so it could be said that if there were to be a difference, *in vivo* physiological loading might have even less breakdown and proteoglycan release than was seen in our unloaded control, and then with loading of stainless-steel implant pins it further increased the proteoglycan release. Many other cartilage wear studies have also used unloaded controls<sup>78,100,139</sup>, and in these early stages it is unlikely a difference in proteoglycan release would be measured between control types.

### 4.3 Future Directions

Normal physiological loading regulates a balance of anabolism and catabolism in the cartilage, but abnormal loading can cause over-expression of MMPs and ADAMTSs<sup>123,139</sup>. Future research directions should include the investigation of MMP and ADAMTS gene expression in response to cartilage wear with different implant curvatures<sup>139</sup>. As mentioned previously, MMP-13, ADAMTS-4, and ADAMTS-5 are known to breakdown proteoglycans and there is much research relating overexpression of these genes to cartilage wear<sup>118,119,123,139</sup>. Our research implied that overexpression of MMPs and ADAMTSs was the likely cause of the delayed increased proteoglycan release reported and it would be beneficial to investigate if there is increasing overexpression in response to increasing RoC.

Further exploration and replication of the surface morphologies of early cartilage wear in response to implant geometry as shown by FESEM is required to solidify implications made in this study and to further understand early wear mechanisms. There are some concerns surrounding the nature of surface ridges and undulations resulting from SEM studies but since this study was comparative, any effects occurring from preparations for

imaging should be consistent across all images<sup>100,140</sup>. Also, investigating proteoglycan release in relation to duration of wear testing would help reveal biological responses of cartilage to wear. Such studies are important for improving our understanding of cartilage wear and implications of hemiarthroplasty implant design.

Future studies could investigate the biological response of human cartilage tissue to hemiarthroplasty implant geometries under identical testing protocols. Similar biological implications as determined from this study would be expected from human cartilage in response to implant geometry.

## 4.4 Conclusions

The findings herein suggest that there is a delayed biological response to cartilage wear that is evident at 72 hours but not at 24 hours after wear testing of 140 minutes. This may be because the proteoglycan release is not an immediate response to mechanical wear but is secondary to increased gene expression of MMPs and ADAMTSs. However, the conformity of hemiarthroplasty implant contact surface had no effect on early biological response at both 24 and 72 hours after the wear testing despite previous literature and our FESEM results having shown decreasing mechanical wear to the cartilage surface with increasing implant RoC, as load is distributed over a greater area. Comparisons between these studies imply that early markers of cartilage wear are primarily mechanical and not biological. Additionally, our results suggest that increased proteoglycan release and FESEM surface changes are early indicators of cartilage damage and occur prior to histological indicators of damage.

Overall, this thesis bridges a gap in our knowledge of the effect hemiarthroplasty implant geometry has on the biological response of early cartilage wear and added to our understanding of wear mechanisms. In bettering our understanding of the underlying factors causing the accelerated cartilage wear reported from hemiarthroplasty implants in patients, we could potentially improve hemiarthroplasty implant designs to improve patient outcomes.

## References

1. Carballo CB, Nakagawa Y, Sekiya I, Rodeo SA. Basic Science of Articular Cartilage. *Clinics in Sports Medicine*. 2017;36(3):413-425.  
doi:10.1016/J.CSM.2017.02.001
2. Lu XL, Mow VC. Biomechanics of articular cartilage and determination of material properties. *Medicine and Science in Sports and Exercise*. Published online 2008. doi:10.1249/mss.0b013e31815cb1fc
3. Varshney M. Articular Cartilage: Structure, Composition and Function. In: *Essential Orthopedics: Principles and Practice (2 Volumes)*. ; 2016.  
doi:10.5005/jp/books/12787\_11
4. Wang Y, Wei L, Zeng L, He D, Wei X. Nutrition and degeneration of articular cartilage. *Knee Surgery, Sports Traumatology, Arthroscopy*. 2013;21(8):1751.  
doi:10.1007/S00167-012-1977-7
5. Akkiraju H, Nohe A. Role of chondrocytes in cartilage formation, progression of osteoarthritis and cartilage regeneration. *Journal of Developmental Biology*. Published online 2015. doi:10.3390/jdb3040177
6. Buckwalter JA, Mankin HJ. Articular cartilage: tissue design and chondrocyte-matrix interactions. *Instr Course Lect*. Published online 1998.
7. Mansour JM, Mow VC. The permeability of articular cartilage under compressive strain and at high pressures. *Journal of Bone and Joint Surgery - Series A*. Published online 1976. doi:10.2106/00004623-197658040-00014
8. Lohmander S. Proteoglycans of joint cartilage. Structure, function, turnover and role as markers of joint disease. *Bailliere's Clinical Rheumatology*. Published online 1988. doi:10.1016/S0950-3579(88)80004-9

9. Hughes C. Kinesiology: The Mechanics and Pathomechanics of Human Movement. *Medicine & Science in Sports & Exercise*. Published online 2004. doi:10.1097/00005768-200403000-00028
10. Khayat A. *Effect of Hemiarthroplasty Implant Contact Geometry and Material on Early Cartilage Wear*. University of Western Ontario; 2015.
11. Boschetti F, Pennati G, Gervaso F, Peretti GM, Dubini G. Biomechanical properties of human articular cartilage under compressive loads. In: *Biorheology*. ; 2004.
12. Mansour JM. Biomechanics of cartilage. In: *Kinesiology: The Mechanics and Pathomechanics of Human Movement: Second Edition*. ; 2013.
13. Radin EL, Burr DB, Caterson B, Fyhrie D, Brown TD, Boyd RD. Mechanical determinants of osteoarthritis. *Seminars in Arthritis and Rheumatism*. Published online 1991. doi:10.1016/0049-0172(91)90036-Y
14. Jin H, Lewis JL. Determination of Poisson's Ratio of Articular Cartilage by Indentation Using Different-Sized Indenters. *Journal of Biomechanical Engineering*. Published online 2004. doi:10.1115/1.1688772
15. Athanasiou KA, Rosenwasser MP, Buckwalter JA, Malinin TI, Mow VC. Interspecies comparisons of in situ intrinsic mechanical properties of distal femoral cartilage. *Journal of Orthopaedic Research*. Published online 1991. doi:10.1002/jor.1100090304
16. Lizhang J, Fisher J, Jin Z, Burton A, Williams S. The effect of contact stress on cartilage friction, deformation and wear. In: *Proceedings of the Institution of Mechanical Engineers, Part H: Journal of Engineering in Medicine*. ; 2011. doi:10.1177/2041303310392626
17. Chen D, Shen J, Zhao W, et al. Osteoarthritis: Toward a comprehensive understanding of pathological mechanism. *Bone Research*. Published online 2017. doi:10.1038/boneres.2016.44

18. Koonce RC, Bravman JT. Obesity and osteoarthritis: More than just wear and tear. *Journal of the American Academy of Orthopaedic Surgeons*. 2013;21(3):161-169. doi:10.5435/JAAOS-21-03-161
19. Jay GD, Waller KA. The biology of Lubricin: Near frictionless joint motion. *Matrix Biology*. Published online 2014. doi:10.1016/j.matbio.2014.08.008
20. CHARNLEY J. The lubrication of animal joints in relation to surgical reconstruction by arthroplasty. *Ann Rheum Dis*. Published online 1960. doi:10.1136/ard.19.1.10
21. Lizhang J, Fisher J, Jin Z, Burton A, Williams S. The effect of contact stress on cartilage friction, deformation and wear. In: *Proceedings of the Institution of Mechanical Engineers, Part H: Journal of Engineering in Medicine*. ; 2011. doi:10.1177/2041303310392626
22. Jay GD, Torres JR, Rhee DK, et al. Association between friction and wear in diarthrodial joints lacking lubricin. *Arthritis and Rheumatism*. Published online 2007. doi:10.1002/art.22974
23. Oungoulian SR, Durney KM, Jones BK, Ahmad CS, Hung CT, Ateshian GA. Wear and damage of articular cartilage with friction against orthopedic implant materials. *Journal of Biomechanics*. Published online 2015. doi:10.1016/j.jbiomech.2015.04.008
24. Chan SMT, Neu CP, Komvopoulos K, Reddi AH, di Cesare PE. Friction and wear of hemiarthroplasty biomaterials in reciprocating sliding contact with articular cartilage. *Journal of Tribology*. Published online 2011. doi:10.1115/1.4004760
25. Lawry G v. Anatomy of Joints, General Considerations, and Principles of Joint Examination. *Musculoskeletal Examination and Joint Injection Techniques*. Published online 2006:1-6. doi:10.1016/B978-0-323-03003-8.50005-2

26. Petty RE, Cassidy JT. Structure and function. *Textbook of Pediatric Rheumatology*. Published online 2005:9-18. doi:10.1016/B978-1-4160-0246-8.50008-5
27. Jay GD, Lane BP, Sokoloff L. Characterization of a bovine synovial fluid lubricating factor III. The interaction with hyaluronic acid. *Connective Tissue Research*. Published online 1992. doi:10.3109/03008209209016818
28. Mow VC, Kuei SC, Lai WM, Armstrong CG. Biphasic creep and stress relaxation of articular cartilage in compression: Theory and experiments. *Journal of Biomechanical Engineering*. Published online 1980. doi:10.1115/1.3138202
29. AP H, TJ J. Challenges associated with using bovine serum in wear testing orthopaedic biopolymers. *Proc Inst Mech Eng H*. 2011;225(10):948-958. doi:10.1177/0954411911416047
30. Morrey BF, An KN. Functional Evaluation of the Elbow. In: *Morrey's The Elbow and Its Disorders*. ; 2009. doi:10.1016/b978-1-4160-2902-1.50010-3
31. An KN, Morrey BF, Chao EYS. The effect of partial removal of proximal ulna on elbow constraint. *Clinical Orthopaedics and Related Research*. Published online 1986. doi:10.1097/00003086-198608000-00041
32. Hotchkiss RN, Weiland AJ. Valgus stability of the elbow. *Journal of Orthopaedic Research*. Published online 1987. doi:10.1002/jor.1100050309
33. King GJW, Morrey BF, An KN. Stabilizers of the elbow. *Journal of Shoulder and Elbow Surgery*. Published online 1993. doi:10.1016/S1058-2746(09)80053-0
34. Burkhart KJ, Nijs S, Mattyasovszky SG, et al. Distal humerus hemiarthroplasty of the elbow for comminuted distal humeral fractures in the elderly patient. *Journal of Trauma - Injury, Infection and Critical Care*. Published online 2011. doi:10.1097/TA.0b013e318216936e



35. Tol MCJM, van den Bekerom MPJ, Sierevelt IN, Hilverdink EF, Raaymakers ELFB, Goslings JC. Hemiarthroplasty or total hip arthroplasty for the treatment of a displaced intracapsular fracture in active elderly patients 12-year follow-up of randomised trial. *Bone and Joint Journal*. Published online 2017. doi:10.1302/0301-620X.99B2.BJJ-2016-0479.R1
36. Blomfeldt R, Törnkvist H, Ericksson K, Söderqvist A, Ponzer S, Tidermark J. A randomised controlled trial comparing bipolar hemiarthroplasty with total hip replacement for displaced intracapsular fractures of the femoral neck in elderly patients. *Journal of Bone and Joint Surgery - Series B*. Published online 2007. doi:10.1302/0301-620X.89B2.18576
37. Baker RP, Squires B, Gargan MF, Bannister GC. Total hip arthroplasty and hemiarthroplasty in mobile, independent patients with a displaced intracapsular fracture of the femoral neck: A randomized, controlled trial. *Journal of Bone and Joint Surgery - Series A*. Published online 2006. doi:10.2106/JBJS.E.01373
38. van Egmond PW, Taminiau AHM, van der Heide HJL. Hemiarthroplasties in young patients with osteonecrosis or a tumour of the proximal femur; An observational cohort study. *BMC Musculoskeletal Disorders*. Published online 2013. doi:10.1186/1471-2474-14-31
39. Eskildsen SM, Kamath G v., del Gaizo DJ. Age matters when comparing hemiarthroplasty and total hip arthroplasty for femoral neck fractures in Medicare patients. *HIP International*. Published online 2019. doi:10.1177/1120700018816924
40. Pace TB, Prather B, Burnikel B, Shirley B, Tanner S, Snider R. Comparative Outcomes Assessment: Hip Hemiarthroplasty as an Alternative to THA in Patients with Surgically Pristine Acetabulum—Is There Still a Role? *ISRN Orthopedics*. Published online 2013. doi:10.1155/2013/632126
41. Yahuaca BI, Simon P, Christmas KN, et al. Acute surgical management of proximal humerus fractures: ORIF vs. hemiarthroplasty vs. reverse shoulder

- arthroplasty. *Journal of Shoulder and Elbow Surgery*. Published online 2020.  
doi:10.1016/j.jse.2019.10.012
42. Antuña SA, Sperling JW, Cofield RH. Shoulder hemiarthroplasty for acute fractures of the proximal humerus: A minimum five-year follow-up. *Journal of Shoulder and Elbow Surgery*. Published online 2008.  
doi:10.1016/j.jse.2007.06.025
43. Boyle MJ, Youn SM, Frampton CMA, Ball CM. Functional outcomes of reverse shoulder arthroplasty compared with hemiarthroplasty for acute proximal humeral fractures. *Journal of Shoulder and Elbow Surgery*. Published online 2013.  
doi:10.1016/j.jse.2012.03.006
44. Levine WN, Fischer CR, Nguyen D, Flatow EL, Ahmad CS, Bigliani LU. Long-term follow-up of shoulder hemiarthroplasty for glenohumeral osteoarthritis. *Journal of Bone and Joint Surgery - Series A*. Published online 2012.  
doi:10.2106/JBJS.K.00603
45. Sperling JW, Cofield RH, Rowland CM. Minimum fifteen-year follow-up of Neer hemiarthroplasty and total shoulder arthroplasty in patients aged fifty years or younger. *Journal of Shoulder and Elbow Surgery*. Published online 2004.  
doi:10.1016/j.jse.2004.03.013
46. Gschwend N. Present state-of-the-art in elbow arthroplasty. *Acta Orthopaedica Belgica*. Published online 2002.
47. Schneeberger AG, Meyer DC, Yian EH. Coonrad-Morrey total elbow replacement for primary and revision surgery: A 2- to 7.5-year follow-up study. *Journal of Shoulder and Elbow Surgery*. Published online 2007.  
doi:10.1016/j.jse.2006.01.013
48. Wright TW, Wong AM, Jaffe R. Functional outcome comparison of semiconstrained and unconstrained total elbow arthroplasties. *Journal of Shoulder and Elbow Surgery*. Published online 2000. doi:10.1067/mse.2000.109408

49. Willing R, Lapner M, King GJW, Johnson JA. In vitro assessment of the contact mechanics of reverse-engineered distal humeral hemiarthroplasty prostheses. *Clinical Biomechanics*. Published online 2014.  
doi:10.1016/j.clinbiomech.2014.08.015
50. van Riet RP, van Glabbeek F, Verborgt O, Gielen J. Capitellar Erosion Caused by a Metal Radial Head Prosthesis: A Case Report. *Journal of Bone and Joint Surgery - Series A*. Published online 2004. doi:10.2106/00004623-200405000-00028
51. Shore BJ, Mozzon JB, MacDermid JC, Faber KJ, King GJW. Chronic posttraumatic elbow disorders treated with metallic radial head arthroplasty. *Journal of Bone and Joint Surgery - Series A*. Published online 2008.  
doi:10.2106/JBJS.F.01535
52. van Glabbeek F, van Riet RP, Baumfeld JA, et al. Detrimental effects of overstuffing or understuffing with a radial head replacement in the medial collateral-ligament deficient elbow. *Journal of Bone and Joint Surgery - Series A*. Published online 2004. doi:10.2106/00004623-200412000-00007
53. Cruess RL, Kwok DC, Duc PN, Lecavalier MA, Dang GT. The response of articular cartilage to weight-bearing against metal. *J Bone Joint Surg Br*. 1984;4:592-597.
54. Cruess RL, Kwok DC, Duc PN, Lecavalier MA, Dang GT. The response of articular cartilage to weight-bearing against metal. *J Bone Joint Surg Br*. 1984;4:592-597.
55. Burkhart KJ, Nijs S, Mattyasovszky SG, et al. Distal humerus hemiarthroplasty of the elbow for comminuted distal humeral fractures in the elderly patient. *Journal of Trauma - Injury, Infection and Critical Care*. Published online 2011.  
doi:10.1097/TA.0b013e318216936e

56. Maghen Y, Leo AJ, Hsu JW, Hausman MR. Is a silastic radial head still a reasonable option? In: *Clinical Orthopaedics and Related Research.* ; 2011. doi:10.1007/s11999-010-1672-2
57. Liew VS, Cooper IC, Ferreira LM, Johnson JA, King GJW. The effect of metallic radial head arthroplasty on radiocapitellar joint contact area. *Clinical Biomechanics*. Published online 2003. doi:10.1016/S0268-0033(02)00172-9
58. Moon KH, Kang JS, Lee TJ, Lee SH, Choi SW, Won MH. Degeneration of acetabular articular cartilage to bipolar hemiarthroplasty. *Yonsei Medical Journal*. Published online 2008. doi:10.3349/ymj.2008.49.5.719
59. Patwari P, Gaschen V, James IE, et al. Ultrastructural quantification of cell death after injurious compression of bovine calf articular cartilage. *Osteoarthritis and Cartilage*. Published online 2004. doi:10.1016/j.joca.2003.11.004
60. Aigner T, McKenna L. Molecular pathology and pathobiology of osteoarthritic cartilage. *Cellular and Molecular Life Sciences*. Published online 2002. doi:10.1007/s00018-002-8400-3
61. Patwari P, Cook MN, DiMicco MA, et al. Proteoglycan degradation after injurious compression of bovine and human articular cartilage in vitro: Interaction with exogenous cytokines. *Arthritis and Rheumatism*. Published online 2003. doi:10.1002/art.10892
62. Giannicola G, Sacchetti FM, Antonietti G, Piccioli A, Postacchini R, Cinotti G. Radial head, radiocapitellar and total elbow arthroplasties: A review of recent literature. *Injury*. Published online 2014. doi:10.1016/j.injury.2013.09.019
63. Mounghondo F, el Kazzi W, van Riet R, Feipel V, Rooze M, Schuind F. Radiocapitellar joint contacts after bipolar radial head arthroplasty. *Journal of Shoulder and Elbow Surgery*. Published online 2010. doi:10.1016/j.jse.2009.09.015

64. Cruess RL, Kwok DC, Duc PN, Lecavalier MA, Dang GT. The response of articular cartilage to weight-bearing against metal. A study of hemiarthroplasty of the hip in the dog. *Journal of Bone and Joint Surgery - Series B*. Published online 1984.
65. Dalldorf PG, Banas MP, Hicks DG, Pellegrini VD. Rate of degeneration of human acetabular cartilage after hemiarthroplasty. *Journal of Bone and Joint Surgery - Series A*. Published online 1995. doi:10.2106/00004623-199506000-00008
66. Calfee R, Madom I, Weiss APC. Radial head arthroplasty. *Journal of Hand Surgery*. Published online 2006. doi:10.1016/j.jhsa.2005.12.005
67. McGann ME, Vahdati A, Wagner DR. Methods to assess in vitro wear of articular cartilage. *Proceedings of the Institution of Mechanical Engineers, Part H: Journal of Engineering in Medicine*. Published online 2012. doi:10.1177/0954411912447014
68. Chan SMT, Neu CP, Komvopoulos K, Reddi AH, di Cesare PE. Friction and wear of hemiarthroplasty biomaterials in reciprocating sliding contact with articular cartilage. *Journal of Tribology*. Published online 2011. doi:10.1115/1.4004760
69. Forster H, Fisher J. The influence of loading time and lubricant on the friction of articular cartilage. *Proceedings of the Institution of Mechanical Engineers, Part H: Journal of Engineering in Medicine*. Published online 1996.
70. Lipshitz H, Etheredge R, Glimcher M. In vitro wear of articular cartilage. *The Journal of Bone & Joint Surgery*. Published online 1975. doi:10.2106/00004623-197557040-00015
71. Luo Y, McCann L, Ingham E, Jin ZM, Ge S, Fisher J. Polyurethane as a potential knee hemiarthroplasty biomaterial: An in-vitro simulation of its tribological performance. *Proceedings of the Institution of Mechanical Engineers, Part H: Journal of Engineering in Medicine*. Published online 2010. doi:10.1243/09544119JEIM657

72. Northwood E, Fisher J. A multi-directional in vitro investigation into friction, damage and wear of innovative chondroplasty materials against articular cartilage. *Clinical Biomechanics*. Published online 2007.  
doi:10.1016/j.clinbiomech.2007.03.008
73. Weightman B. In vitro fatigue testing of articular cartilage. *Ann Rheum Dis*. Published online 1975.
74. Torzilli PA, Grigiene R, Borrelli J, Helfet DL. Effect of impact load on articular cartilage: cell metabolism and viability, and matrix water content. *J Biomech Eng*. 1999;121(5):433-441.
75. McCann L, Ingham E, Jin Z, Fisher J. Influence of the meniscus on friction and degradation of cartilage in the natural knee joint. *Osteoarthritis and Cartilage*. Published online 2009. doi:10.1016/j.joca.2009.02.012
76. McCann L, Ingham E, Jin Z, Fisher J. An investigation of the effect of conformity of knee hemiarthroplasty designs on contact stress, friction and degeneration of articular cartilage: A tribological study. *Journal of Biomechanics*. Published online 2009. doi:10.1016/j.jbiomech.2009.03.028
77. Dedecker S. *The Efficacy of Bionate as an Articulating Surface for Joint Hemiarthroplasty*. University of Western Ontario; 2017.
78. Verberne G, Merkher Y, Halperin G, Maroudas A, Etsion I. Techniques for assessment of wear between human cartilage surfaces. *Wear*. 2009;266:1216-1223.  
doi:10.1016/j.wear.2009.03.042
79. Rutgers M, van Pelt MJP, Dhert WJA, Creemers LB, Saris DBF. Evaluation of histological scoring systems for tissue-engineered, repaired and osteoarthritic cartilage. *Osteoarthritis and Cartilage*. Published online 2010.  
doi:10.1016/j.joca.2009.08.009

80. Oungouljian SR, Chang S, Bortz O, et al. Articular cartilage wear characterization with a particle sizing and counting analyzer. *Journal of Biomechanical Engineering*. Published online 2013. doi:10.1115/1.4023456
81. Guilak F, Meyer BC, Ratcliffe A, Mow VC. The effects of matrix compression on proteoglycan metabolism in articular cartilage explants. *Osteoarthritis and Cartilage*. Published online 1994. doi:10.1016/S1063-4584(05)80059-7
82. Farndale RW, Buttle DJ, Barrett AJ. Improved quantitation and discrimination of sulphated glycosaminoglycans by use of dimethylmethylene blue. *BBA - General Subjects*. Published online 1986. doi:10.1016/0304-4165(86)90306-5
83. Lipshitz H, Glimcher MJ. In vitro studies of the wear of articular cartilage II. Characteristics of the wear of articular cartilage when worn against stainless steel plates having characterized surfaces. *Wear*. Published online 1979. doi:10.1016/0043-1648(79)90070-X
84. Hu Q, Ecker M. Overview of MMP-13 as a Promising Target for the Treatment of Osteoarthritis. *International Journal of Molecular Sciences*. 2021;22(4):1-22. doi:10.3390/IJMS22041742
85. Wang M, Sampson ER, Jin H, et al. MMP13 is a critical target gene during the progression of osteoarthritis. *Arthritis Research and Therapy*. Published online 2013. doi:10.1186/ar4133
86. Barrett AJ, Rawlings ND, Woessner JF. Handbook of Proteolytic Enzymes: Second Edition. *Handbook of Proteolytic Enzymes: Second Edition*. 2004;1:1-1140. doi:10.1016/C2009-0-03628-9
87. Verma P, Dalal K. ADAMTS-4 and ADAMTS-5: key enzymes in osteoarthritis. *J Cell Biochem*. 2011;112(12):3507-3514. doi:10.1002/JCB.23298
88. Dancevic CM, McCulloch DR. Current and emerging therapeutic strategies for preventing inflammation and aggrecanase-mediated cartilage destruction in

- arthritis. *Arthritis Research and Therapy*. 2014;16(5):1-11. doi:10.1186/S13075-014-0429-9/TABLES/2
89. Yatabe T, Mochizuki S, Takizawa M, et al. Hyaluronan inhibits expression of ADAMTS4 (aggrecanase-1) in human osteoarthritic chondrocytes. *Annals of the Rheumatic Diseases*. 2009;68(6):1051-1058. doi:10.1136/ARD.2007.086884
90. Huang K, Wu LD. Aggrecanase and Aggrecan degradation in osteoarthritis: A review. *Journal of International Medical Research*. 2008;36(6):1149-1160. doi:10.1177/147323000803600601
91. Malfait AM, Liu RQ, Ijiri K, Komiya S, Tortorella MD. Inhibition of ADAM-TS4 and ADAM-TS5 prevents aggrecan degradation in osteoarthritic cartilage. *J Biol Chem*. 2002;277(25):22201-22208. doi:10.1074/JBC.M200431200
92. Mankin HJ, Dorfman H, Lippiello L, Zarins A. Biochemical and metabolic abnormalities in articular cartilage from osteo-arthritic human hips. II. Correlation of morphology with biochemical and metabolic data. *J Bone Joint Surg Am*. Published online 1971. doi:10.2106/00004623-197153030-00009
93. Waldstein W, Perino G, Gilbert SL, Maher SA, Windhager R, Boettner F. OARSI osteoarthritis cartilage histopathology assessment system: A biomechanical evaluation in the human knee. *Journal of Orthopaedic Research*. Published online 2016. doi:10.1002/jor.23010
94. Pritzker KPH, Gay S, Jimenez SA, et al. Osteoarthritis cartilage histopathology: Grading and staging. *Osteoarthritis and Cartilage*. Published online 2006. doi:10.1016/j.joca.2005.07.014
95. Pauli C, Whiteside R, Heras FL, et al. Comparison of cartilage histopathology assessment systems on human knee joints at all stages of osteoarthritis development. *Osteoarthritis and Cartilage*. Published online 2012. doi:10.1016/j.joca.2011.12.018



96. Hossain MJ, Noori-Dokht H, Karnik S, et al. Anisotropic properties of articular cartilage in an accelerated in vitro wear test. *Journal of the Mechanical Behavior of Biomedical Materials*. Published online 2020.  
doi:10.1016/j.jmbbm.2020.103834
97. Trevino RL, Stoia J, Laurent MP, Pacione CA, Chubinskaya S, Wimmer MA. Establishing a live cartilage-on-cartilage interface for tribological testing. *Biotribology*. Published online 2017. doi:10.1016/j.biotri.2016.11.002
98. Wimmer MA, Pacione C, Yuh C, et al. Articulation of an alumina-zirconia composite ceramic against living cartilage – An in vitro wear test. *Journal of the Mechanical Behavior of Biomedical Materials*. Published online 2020.  
doi:10.1016/j.jmbbm.2019.103531
99. Cruz R, Ramírez C, Rojas OI, Casas-Mejía O, Kouri JB, Vega-López MA. Menisectomized miniature Vietnamese pigs develop articular cartilage pathology resembling osteoarthritis. *Pathology Research and Practice*. Published online 2015. doi:10.1016/j.prp.2015.07.012
100. Graindorge SL, Stachowiak GW. Changes occurring in the surface morphology of articular cartilage during wear. *Wear*. Published online 2000. doi:10.1016/S0043-1648(00)00386-0
101. Forster H, Fisher J. The influence of continuous sliding and subsequent surface wear on the friction of articular cartilage. *Proceedings of the Institution of Mechanical Engineers, Part H: Journal of Engineering in Medicine*. Published online 1999. doi:10.1243/0954411991535167
102. Clark JM, Simonian PT. Scanning electron microscopy of “fibrillated” and “malacic” human articular cartilage: Technical considerations. *Microscopy Research and Technique*. Published online 1997. doi:10.1002/(SICI)1097-0029(19970515)37:4<299::AID-JEMT5>3.0.CO;2-G

103. Podsiadlo P, Stachowiak GW. Numerical analysis of shape of wear particles from arthritic and asymptomatic synovial joints. *Journal of Orthopaedic Rheumatology*. Published online 1995.
104. Langohr GG, Willing R, Medley JB, King GJ, Johnson JA. Finite element contact analysis of axisymmetric and non-axisymmetric radial head hemiarthroplasty. *Orthopaedic Research Society Annual Meeting*. Published online 2013.
105. Lalone EA, McDonald CP, Ferreira LM, Peters TM, King GW, Johnson JA. Development of an image-based technique to examine joint congruency at the elbow. *Comput Methods Biomech Biomed Engin*. 2013;16(3):280-290.
106. Brandt JM. *Wear and Boundary Lubrication in Modular Total Knee Replacements*. 2008.
107. Ltd B. Blyscan™ Sulfated Glycosaminoglycan Assay. Accessed December 21, 2021. [www.biocolor.co.uk](http://www.biocolor.co.uk)
108. Glycosaminoglycan Assay | Blyscan™ | Biocolor - [biocolor.co.uk](http://biocolor.co.uk). Accessed November 1, 2021. <https://www.biocolor.co.uk/product/blyscan-glycosaminoglycan-assay/>
109. *Blyscan Sulfated Glycosaminoglycan Assay*.; 2016. <https://www.biocolor.co.uk/site/wp-content/uploads/2016/04/blyscan-assay-manual-1.pdf>
110. Wall A, Board T. Chemical Basis for the Histological Use of Safranin O in the Study of Articular Cartilage. *Classic Papers in Orthopaedics*. Published online January 1, 2014:433-435. doi:10.1007/978-1-4471-5451-8\_110
111. KL C, SA A. Limitations of safranin “O” staining in proteoglycan-depleted cartilage demonstrated with monoclonal antibodies. *Histochemistry*. 1988;89(2):185-188. doi:10.1007/BF00489922

112. Pandithage R. Brief Introduction to Critical Point Drying. Published online December 10, 2012.
113. Eckstein F, Cicuttini F, Raynauld JP, Waterton JC, Peterfy C. Magnetic resonance imaging (MRI) of articular cartilage in knee osteoarthritis (OA): morphological assessment. *Osteoarthritis and Cartilage*. 2006;14(SUPPL. 1):46-75. doi:10.1016/J.JOCA.2006.02.026
114. Schmitz RJ, Wang HM, Polprasert DR, Kraft RA, Pietrosimone BG. Evaluation of knee cartilage thickness: A comparison between ultrasound and magnetic resonance imaging methods. Published online 2016. doi:10.1016/j.knee.2016.10.004
115. Eckstein F, Collins JE, Nevitt MC, et al. CARTILAGE THICKNESS CHANGE AS AN IMAGING BIOMARKER OF KNEE OSTEOARTHRITIS PROGRESSION – DATA FROM THE FNIH OA BIOMARKERS CONSORTIUM. *Arthritis Rheumatol*. 2015;67(12):3184. doi:10.1002/ART.39324
116. Bertrand J, Held A. Role of Proteoglycans in Osteoarthritis. *Cartilage: Volume 2: Pathophysiology*. Published online January 1, 2017:63-80. doi:10.1007/978-3-319-45803-8\_4
117. Handley CJ, Lowther DA, McQuillan DJ. The structure and synthesis of proteoglycans of articular cartilage. *Cell Biol Int Rep*. 1985;9(9):753-782. doi:10.1016/0309-1651(85)90095-5
118. Wang M, Sampson ER, Jin H, et al. MMP13 is a critical target gene during the progression of osteoarthritis. *Arthritis Research and Therapy*. 2013;15(1):1-11. doi:10.1186/AR4133/FIGURES/4
119. Majumdar MK, Askew R, Schelling S, et al. Double-knockout of ADAMTS-4 and ADAMTS-5 in mice results in physiologically normal animals and prevents the progression of osteoarthritis. *Arthritis Rheum*. 2007;56(11):3670-3674. doi:10.1002/ART.23027

120. Roughley PJ, Mort JS. The role of aggrecan in normal and osteoarthritic cartilage. *Journal of Experimental Orthopaedics*. 2014;1(1):1-11. doi:10.1186/S40634-014-0008-7
121. Kiani C, Chen L, Wu YJ, Yee AJ, Yang BB. Structure and function of aggrecan. *Cell Research 2002 12:1*. 2002;12(1):19-32. doi:10.1038/sj.cr.7290106
122. Schaetti OR, Schaetti S, Gallo LM, Torzilli PA. A Model to Study Articular Cartilage Mechanical and Biological Responses to Sliding Loads. *Annals of Biomedical Engineering*. 44. doi:10.1007/s10439-015-1543-9
123. Lee JH, Fitzgerald JB, DiMicco MA, Grodzinsky AJ. Mechanical injury of cartilage explants causes specific time-dependent changes in chondrocyte gene expression. *Arthritis Rheum*. 2005;52(8):2386-2395. doi:10.1002/ART.21215
124. Springer BD, Scott RD, Sah AP, Carrington R. McKeever hemiarthroplasty of the knee in patients less than sixty years old. *Journal of Bone and Joint Surgery - Series A*. 2006;88(2):366-371. doi:10.2106/JBJS.E.00123
125. Springer BD, Scott RD, Sah AP, Carrington R. McKeever hemiarthroplasty of the knee in patients less than sixty years old. *J Bone Joint Surg Am*. 2006;88(2):366-371. doi:10.2106/JBJS.E.00123
126. McCann L, Ingham E, Jin Z, Fisher J. An investigation of the effect of conformity of knee hemiarthroplasty designs on contact stress, friction and degeneration of articular cartilage: A tribological study. *Journal of Biomechanics*. 2009;42(9):1326-1331. doi:10.1016/J.JBIOMECH.2009.03.028
127. Desai SJ, Lalone E, Athwal GS, Ferreira LM, Johnson JA, King GJW. Hemiarthroplasty of the elbow: the effect of implant size on joint congruency. *Journal of Shoulder and Elbow Surgery*. 2016;25(2):297-303. doi:10.1016/J.JSE.2015.09.022
128. Ghallab A. In vitro test systems and their limitations. *EXCLI Journal*. 2013;12:1024. doi:10.17877/DE290R-7558

129. Trevino RL, Stoia J, Laurent MP, Pacione CA, Chubinskaya S, Wimmer MA. Establishing a live cartilage-on-cartilage interface for tribological testing. *Biotribology*. 2017;9:1-11. doi:10.1016/J.BIOTRI.2016.11.002
130. Nickien M, Heuijerjans A, Ito K, van Donkelaar CC. Comparison between in vitro and in vivo cartilage overloading studies based on a systematic literature review. *Journal of Orthopaedic Research*. 2018;36(8):2076. doi:10.1002/JOR.23910
131. Lunney JK, Goor A van, Walker KE, Hailstock T, Franklin J, Dai C. Importance of the pig as a human biomedical model. *Science Translational Medicine*. 2021;13(621). doi:10.1126/SCITRANSLMED.ABD5758
132. Vodička P, Jr KS, ... BDA of the N, 2005 undefined. The miniature pig as an animal model in biomedical research. *researchgate.net*. Published online 2005. doi:10.1196/annals.1334.015
133. Torzilli PA, Deng XH, Ramcharan M. Effect of compressive strain on cell viability in statically loaded articular cartilage. *Biomechanics and Modeling in Mechanobiology*. 2006;5(2-3):123-132. doi:10.1007/S10237-006-0030-5
134. Levin AS, Chen CTC, Torzilli PA. Effect of tissue maturity on cell viability in load-injured articular cartilage explants. *Osteoarthritis and Cartilage*. 2005;13(6):488-496. doi:10.1016/J.JOCA.2005.01.006
135. Olivier P, Loeuille D, Watrin A, et al. Structural Evaluation of Articular Cartilage Potential Contribution of Magnetic Resonance Techniques Used in Clinical Practice. *ARTHRITIS & RHEUMATISM*. 2001;44(10):2285-2295. doi:10.1002/1529-0131
136. Otterness IG, Eckstein F. Women have thinner cartilage and smaller joint surfaces than men after adjustment for body height and weight. *Osteoarthritis and Cartilage*. 2007;15(6):666-672. doi:10.1016/J.JOCA.2006.12.003
137. Faber SC, Eckstein F, Lukasz S, et al. Gender differences in knee joint cartilage thickness, volume and articular surface areas: assessment with quantitative three-

dimensional MR imaging. *Skeletal Radiol.* 2001;30(3):144-150.

doi:10.1007/S002560000320

138. McDonnell AC, Eiken O, Mekjavic IB, Žlak N, Drobnič M. The influence of a sustained 10-day hypoxic bed rest on cartilage biomarkers and subchondral bone in females: The FemHab study. *Physiological Reports.* 2020;8(8):e14413.  
doi:10.14814/PHY2.14413
139. Scha'tti OR, Scha'tti S, Gallo LM, Torzilli PA. A Model to Study Articular Cartilage Mechanical and Biological Responses to Sliding Loads. *Annals of Biomedical Engineering.* 44. doi:10.1007/s10439-015-1543-9
140. Bloebaum RD, Wilson AS. The morphology of the surface of articular cartilage in adult rats. *J Anat.* Published online 1980.

## Appendices

### Appendix A – Glossary

ADAMTSs	A Disintegrin and Metalloproteinase with Thrombospondin motifs. A family of multidomain extracellular protease enzymes.
Anabolic	Relating to or promoting anabolism. A set of metabolic pathways that construct molecules from smaller units.
Arthroplasty	A surgical procedure restoring joint function.
Assay	An analysis performed to determine the presence and amount of a substance.
Catabolic	Relating to or promoting catabolism. Metabolic activity concerned with the breakdown of complex molecules.
Chondrocytes	The only cells found in healthy cartilage.
Culture medium	Any solid, liquid, or semi-solid designed specifically to support the growth, storage, or transport of a population of microorganisms or cells.
Extracellular matrix	An intricate, three-dimensional, tissue-specific network made of an array of structural and functional proteins.

Fissure	A split or crack forming a long narrow opening.
Glycosaminoglycans	Long linear polysaccharides with repeating disaccharide (two-sugar) units.
Hemiarthroplasty	A surgical procedure replacing one articulating surface with an implant to restore joint function.
Histology	Microscopic anatomy. A branch of biology studying the microanatomy of tissues.
<i>In vitro</i>	Latin: “within the glass”. A process or experiment happening outside of a living organism.
<i>In vivo</i>	Latin: “within the living”. A process or experiment conducted inside of a living organism.
Medical implant	A device or tissue placed inside/on the surface of the body. Most are prosthetics intended to replace body parts.
Matrix metalloproteinases	Metalloproteinases that are zinc-dependent proteolytic enzymes that degrade various proteins in the extracellular matrix.
Morphology	A branch of biology that looks at the form and structure of organisms.



Osteoarthritis	A joint disease characterised by the degeneration of articular cartilage which results in bone stiffening and reduces joint functionality.
Proteoglycan	A core protein with one or more covalently attached glycosaminoglycan chain(s).
Striations	A series of parallel ridges, furrows, or linear marks.
Surface morphology	A subset of analytical imaging. A qualitative evaluation of the three-dimensional shape of a surface.
Undulations	A continuous up and down shape or movement.
Wear	Damage, erosion, or deterioration by friction.

## Appendix B – Pilot Studies for Time Point and Concentration Optimization

Pilot studies were conducted assessing proteoglycan concentration in the pooled media at 0, 12, and 24 hours after wear testing. Optimal dilution schemes were also assessed.

**Table B-1:** *The treatments applied to each sample in the pilot studies.*

*Samples S1-S4 underwent the same testing conditions using a 4.70mm pin, left for 24 hours after wear testing, and then were concentrated/diluted to different amounts.*

*Samples S1, S5, and S6 underwent the same testing conditions using a 4.70mm pin, were not concentrated/diluted, and were left for different amounts of time after wear testing (24, 0, 12 hours, respectively).*

*Samples S2 and S7 were worn using different pin geometries (4.70mm and 11.70mm, respectively) under the same testing conditions, were left for 24 hours after testing, and were not concentrated/diluted.*

Sample Number	RoC (mm)	Time Point (hours)	Dilution Scheme
S1	4.70	24	50µL Sample + 50 µL DI Water
S2	4.70	24	100 µL Sample (no dilution)
S3	4.70	24	Concentrated 2-fold 50 µL Sample + 50 µL DI Water
S4	4.70	24	Concentrated 2-fold 100 µL Sample (no dilution)
S5	4.70	0	100 µL Sample (no dilution)
S6	4.70	12	100 µL Sample (no dilution)
S7	11.70	24	100 µL Sample (no dilution)

Figure B-1 below shows results of the above sample numbers (S1-S7) plotted along a calibration curve. All samples had concentrations in the lower quarter of the calibration curve and so it was determined that samples would need to be concentrated more (8x) to fall around the center of the calibration curve (between standards 1-4). These pilot studies showed that the 24-hour time point had a higher proteoglycan concentration than at 0 and 12 hours after wear.

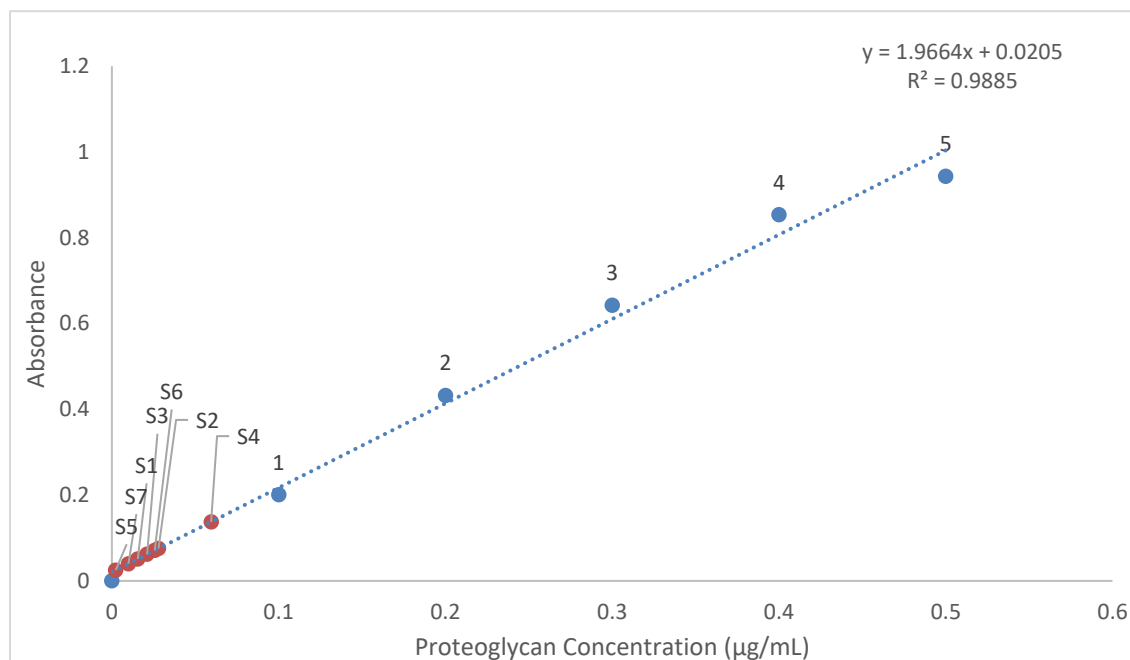


**Figure B-1:** Plot of pilot studies assessing proteoglycan concentrations at 0, 12, and 24 hours after wear testing, different concentrations/dilutions, and pin geometries.

Points 1-5 represent proteoglycan standards of known concentrations 0.1-0.5µg and were used to form the line of best fit  $y = 1.9664x + 0.0205$ .  $R^2 = 0.9885$ .

## Curriculum Vitae

**Name:** Debora Rossetti

**Post-secondary** University of Western Ontario

**Education and** London, Ontario, Canada

**Degrees:** 2015-2019 B.Sc. Biology & Chemistry

University of Western Ontario

London, Ontario, Canada

2019-2022 M.E.Sc. Biomedical Engineering

*Collaborative Specialization in Musculoskeletal Health Research*

**Honours and** Dean's Honour List

**Awards:** 2015, 2019

**Related Work** Teaching Assistant

**Experience** University of Western Ontario

2019-2021